

BWRVIP

BWR Vessel & Internals Project _____ 2000-114

April 14, 2000

Document Control Desk
U. S. Nuclear Regulatory Commission
11555 Rockville Pike
Rockville, MD 20852

Attention: C. E. Carpenter

Subject: Project 704 - Transmittal of "BWR Vessel and Internals Project, Evaluation of Stress Corrosion Crack Growth in Low Alloy Steel Vessel Materials in the BWR Environment (BWRVIP-60NP)," EPRI Report TR-108709NP, April 2000.

Reference: Letter from C. Terry to C. E. Carpenter, March 30, 1999: Transmittal of "BWR Vessel and Internals Project, Evaluation of Stress Corrosion Crack Growth in Low Alloy Steel Vessel Materials in the BWR Environment (BWRVIP-60)," EPRI Report TR-108709, March 1999.

Enclosed are two (2) copies of the subject report. This is the non-proprietary version of the document submitted to the NRC by the letter referenced above.

If you have any questions on this subject please call Steve Lewis of Entergy, BWRVIP Assessment Committee Chairman, at (601) 368-5444.

Sincerely,



Carl Terry
Niagara Mohawk Power Company
Chairman, BWR Vessel and Internals Project

Enclosure

D058

BWR Vessel and Internals Project Evaluation of Stress Corrosion Crack Growth in Low Alloy Steel Vessel Materials in the BWR Environment (BWRVIP-60NP)

NON-PROPRIETARY INFORMATION

NOTICE: This report contains the non-proprietary information that is included in the proprietary version of this report. The proprietary version of this report contains proprietary information that is the intellectual property of BWRVIP utility members and EPRI. Accordingly, the proprietary report is available only under license from EPRI and may not be reproduced or disclosed, wholly or in part, by any Licensee to any other person or organization.

REPORT SUMMARY

The Boiling Water Reactor Vessel and Internals Project (BWRVIP), formed in June 1994, is an association of utilities focused exclusively on BWR vessel and internals materials issues. This report, provides a methodology for assessing crack growth in BWR low alloy steel pressure vessels and nozzles.

Background

Events in 1993 and 1994 involving the core shroud confirmed that intergranular stress corrosion cracking (IGSCC) is a significant issue for austenitic materials used in BWR internals. Following the initial evidence of IGSCC, US BWR utilities formed the BWRVIP in June 1994, to address integrity issues arising from service related degradation of key BWR internals components.

In addition to the vessel internals concerns, the BWRVIP has developed a methodology for evaluating long-term integrity of the RPVs in BWR plants, in particular with regard to potential susceptibility of the austenitic cladding or the LAS base metal to SCC during operation. Whereas the field experience with the LAS plate and nozzle materials in the BWR environment has been excellent, there have been a limited number on incidents where cracking has initiated in weldments attached to nozzle butter or where vessel cladding cracks have come into contact with the underlying vessel materials.

Objective

- To formalize a methodology for determination of stress corrosion crack growth into low alloy steel vessels and nozzles in BWRs.
- To develop the operational and residual stresses and associated fracture mechanics stress intensity factors (K) at key vessel locations to estimate the SCC crack growth behavior in LAS components.

Approach

The approach used was to examine the history of SCC in LAS components in the BWR and to evaluate the current state of understanding of SCC in these materials based upon laboratory data. Based upon existing crack growth rate data and the mechanistic understanding, an interim crack growth disposition curve has been developed. The disposition curve has both a K-dependent and K-independent portion which are chosen based on water chemistry condition and K level. Through-wall residual stress distributions were obtained on a generic basis for the vessel cladding, attachment welds and vessel welds. Operating stresses vary from plant to plant and can be

obtained from the plant's stress report. Various fracture mechanics models were used to determine the through-wall stress intensity factor (K) distributions for the cladding, attachment and vessel welds. The crack growth law and the K distributions can be used to determine the time for an initial flaw to reach the ASME Section XI allowable flaw size for the vessel location of interest.

Results

Example problems were performed for circumferential and axial flaws in the vessel head and in the vessel around the vicinity of the shroud support plate to vessel weld (H9) in a BWR environment using the crack growth rate-stress intensity distributions developed in this study. The evaluation results indicate that for both types of flaws, considerable time exists for initial through-clad flaws to reach the ASME Section XI allowable flaw size, thereby demonstrating the substantial flaw tolerance in BWR pressure vessels. It is further noted that a comprehensive industry database of service-induced cracking has shown that no SCC induced damage has occurred in BWR RPVs, thereby demonstrating the conservatism of this methodology.

EPRI Perspective

The results of this study reveal that low alloy steel RPVs are extremely tolerant to postulated SCC cracks emanating from attachment welds or weld metal cladding. The field and laboratory data illustrate that crack initiation and growth is extremely difficult and that no SCC induced damage has been observed in BWR vessel components. All cracking observed has been in cladding and most of the cracking was the result of a manufacturing or fabrication defect. Even when limited environmentally assisted corrosion has been observed in vessel cladding, it has arrested at the vessel-clad interface. This result indicates that the consideration of possible SCC growth into the LAS is, in fact, conservative.

TR-108709NP

Interest Categories

Piping, Reactor, Vessel and Materials
Licensing and Safety Assessment

Key Words

Boiling Water Reactor
Reactor Pressure Vessel
Crack Growth Rate
Residual Stresses
Stress Corrosion Cracking
Low Alloy Steels

BWR Vessel and Internals Project

Evaluation of Stress Corrosion Crack Growth in Low Alloy Steel Vessel Materials in the BWR Environment (BWRVIP-60NP)

TR-108709 NP
Research Project WOB301-45

Final Report, March 2000

Prepared by:

STRUCTURAL INTEGRITY ASSOCIATES, INC.
3315 Almaden Expressway, Suite 24
San Jose, CA 95118-1557

in Collaboration with

GE Nuclear Energy
Modeling and Computing Services
Entergy Operations, Inc.
EPRI Repair and Replacement Center
Berkeley Research and Engineering
Dominion Engineering, Inc.
Corrosion & Materials Consultancy

Prepared for

**BOILING WATER REACTOR VESSEL & INTERNALS PROJECT and
EPRI**

3412 Hillview Ave.
Palo Alto, California 94304

DISCLAIMER OF WARRANTIES AND LIMITATION OF LIABILITIES

This report was prepared by the organization(s) named below as an account of work sponsored or cosponsored by the BWR Vessel and Internals Project (BWRVIP) and the Electric Power Research Institute, Inc. (EPRI). Neither BWRVIP, EPRI, any member of EPRI, any cosponsor, the organization(s) named below, nor any person acting on behalf of any of them:

(a) makes any warranty or representation whatsoever, express or implied, (i) with respect to the use of any information, apparatus, method, process or similar item disclosed in this report, including merchantability and fitness for a particular purpose, or (ii) that such use does not infringe on or interfere with privately owned rights, including any party's intellectual property, or (iii) that this report is suitable to any particular user's circumstance, or

(b) assumes any responsibility for any damages or other liability whatsoever (including any consequential damages, even if BWRVIP, EPRI or any EPRI representative has been advised of the possibility of such damages) resulting from your selection or use of this report or any information, apparatus, method, process or similar item disclosed in this report.

Organization(s) that prepared this report:

STRUCTURAL INTEGRITY ASSOCIATES, INC.

in Collaboration with

GE Nuclear Energy

Modeling and Computing Services

Entergy Operations, Inc.

EPRI Repair and Replacement Center

Berkeley Research and Engineering

Dominion Engineering, Inc.

Corrosion & Materials Consultancy

ORDERING INFORMATION

Requests for copies of this report should be directed to the BWRVIP Program Manager, 3412 Hillview Ave., Palo Alto, CA 94304, (650) 855-2340.

Acknowledgments

The members of the BWRVIP Crack Growth Working Group, listed below, are gratefully acknowledged for their efforts which led to the successful completion of this document.

Dana Covill	General Public Utilities
Jai Brihmadesan	Entergy Operations
George Inch	Niagara Mohawk Power Corp.
Tony Giannuzzi	Structural Integrity Associates
Ron Horn	GE Nuclear Energy
Dave Morgan	Pennsylvania Power and Light
Larry Nelson	EPRI
Raj Pathania (Project Manager)	EPRI
John Wilson	Illinois Power
Steve Leshnoff	General Public Utilities
Ed Hartwig	Tennessee Valley Authority
John Grimm	FirstEnergy Corp
Bob Carter	EPRI

Principal Authors:

N. G. Cofie	Structural Integrity Associates
A. J. Giannuzzi	Structural Integrity Associates
D. E. Delwiche	Structural Integrity Associates
B. M. Gordon	Structural Integrity Associates
R. Horn	GE Nuclear Energy
P. Ford	GE CR & D
W. Cheng	Bear Inc. (Formerly UC Berkeley)
A. P. L. Turner	Dominion Engineering, Inc.
J. Broussard	Dominion Engineering, Inc.
J. Hickling	Corrosion & Materials Consultancy
A. Peterson	EPRI Repair and Replacement Center

Table of Contents

<u>Section</u>	<u>Page</u>
1.0 INTRODUCTION.....	1-1
2.0 RPV CONFIGURATIONS AND VESSEL ATTACHMENT TYPES AND LOCATIONS.....	2-1
2.1 BWR Vessel Configurations	2-1
2.2 Classification of Attachment Welds.....	2-3
2.3 References	2-4
3.0 OPERATING EXPERIENCE WITH PRESSURE VESSELS IN BWR PLANTS RELATED TO ENVIRONMENTALLY ASSISTED CRACKING WITH PARTICULAR EMPHASIS ON STRESS CORROSION CRACKING	3-1
3.1 Introduction	3-1
3.2 Research Reactors	3-2
3.2.1 Elk River, USA.....	3-2
3.2.2 Argonne EBWR, USA,	3-2
3.2.3 JPDR, Tokai, Japan	3-3
3.3 BWRs in Commercial Operation	3-5
3.3.1 Feedwater Nozzle Cracking in US Design BWRs.....	3-5
3.3.2 Inlet nozzle safe end cracking (Alloy 182 cladding).....	3-9
3.3.3 Inlet nozzle cracking (Alloy 182 cladding)	3-10
3.3.4 EAC in the Feedwater Pipe to Nozzle Weld of a non-US Design BWR.....	3-11
3.3.5 Reactor vessel head cracking (heads clad with austenitic stainless steel)	3-13
3.3.6 Reactor vessel head cracking (unclad head).....	3-17
3.3.7 Damage to another BWR Pressure Vessel (Steam Converter)	3-18
3.4 Overall Assessment and Conclusion	3-20
3.4.1 Austenitic Stainless Steel Cladding.....	3-21
3.4.2 Low-alloy Steel Base Material	3-21
3.5 References	3-23
4.0 STRESS CORROSION CRACKING OF LOW ALLOY STEEL IN BWR WATER: LABORATORY STUDIES	4-1
4.1 Old Laboratory Results from GENE.....	4-1
4.2 Previous Results from GENE GE CR&D: EPRI RP C102-4	4-2
4.3 Recent Reactor Site Testing Data.....	4-4
4.4 Other Testing Results	4-6
4.5 Summary of Test Results	4-9
4.6 References	4-13
5.0 CURRENT CRACK PROPAGATION RATE/STRESS INTENSITY DISPOSITION RELATIONSHIPS AND THEIR DERIVATION.....	5-1
5.1 Working Hypothesis for the Stress Corrosion Cracking Mechanism in the Low-Alloy Steel/Water System at 288 C (550 F): Film Rupture/Slip-Oxidation Mechanism	5-1

Table of Contents (concluded)

<u>Section</u>	<u>Page</u>
5.2 Development of the High Sulfur and Low Sulfur Crack Growth Prediction Algorithms for Low-Alloy Steel/Water Systems at 288° C (550° F)	5-2
5.3 Comparison of Observed and Predicted Stress Corrosion Crack Propagation Rates in LAS/Water Systems At 288° C (550° F)	5-4
5.4 Interim Recommendations on Disposition Relationships	5-6
5.4.1 <i>Basis for Disposition Line Positioning</i>	5-6
5.4.2 <i>Disposition Line: Constant Load</i>	5-7
5.4.3 <i>Disposition Line: Water Chemistry and Load Transients</i>	5-8
5.5 References	5-9
6.0 OPERATIONAL AND RESIDUAL STRESS DETERMINATION, AND FRACTURE MECHANICS CONSIDERATIONS.....	6-1
6.1 Vessel Clad Residual Stresses.....	6-1
6.2 Attachment Weld Residual Stresses.....	6-4
6.2.1 <i>Attachment Welds and Pads Welded to the Cladding</i>	6-4
6.2.2 <i>Nickel Alloy Pad Attachment Weld</i>	6-5
6.3 Vessel Weld Residual.....	6-6
6.4 Operating Stresses	6-6
6.5 Fracture Mechanics Stress Intensity Factor Considerations	6-7
6.5.1 <i>Axial Flaws</i>	6-8
6.5.2 <i>Circumferential Flaws</i>	6-9
6.6 References	6-11
7.0 EXAMPLES OF FRACTURE MECHANICS METHODOLOGY FOR RPV AND ATTACHMENTS	7-1
7.1 Top Head Cracking Evaluation – Clad Crack Growth Example (Circumferential Flaw).....	7-1
7.1.1 <i>Background</i>	7-1
7.1.2 <i>Stresses</i>	7-2
7.1.3 <i>Stress Intensity Factors</i>	7-3
7.1.4 <i>Stress Corrosion Crack Growth Evaluation</i>	7-4
7.1.5 <i>Allowable Flaw Size</i>	7-5
7.2 H-9 Attachment Weld – Crack Growth Example (Circumferential Flaw)	7-6
7.2.1 <i>Background</i>	7-6
7.2.2 <i>Stresses</i>	7-6
7.2.3 <i>Stresses Intensity Factors</i>	7-7
7.2.4 <i>Stress Corrosion Crack Growth Evaluation</i>	7-8
7.3 Examples with Axial Flaws.....	7-8
7.4 References	7-9
8.0 SUMMARY and CONCLUSIONS	8-1
APPENDIX A: EPRI RPC102-4: Stress Corrosion Cracking in Low Alloy Steels	A-1

List of Tables

<u>Table</u>	<u>Page</u>
Table 2-1 Design Information for GE Nuclear Energy Reactor Vessels [2-1]	2-5
Table 2-2 Clad to Thickness Ratios for Typical Reactor Vessels [2-2].....	2-6
Table 2-3 Summary of Attachment Welds [2-2].....	2-7
Table 3-1 Ultrasonic indications at Brunswick Unit 1 recirc inlet safe-end-to-nozzle welds [3-10]	3-25
Table 3-2 Overview of RPV degradation in BWR-Plants	3-26
Table 4-1 Test Results: RP C1024 Appendix III: GE Nuclear Energy Six Specimen Test.....	4-14
Table 4-2 Summary of Different Test Time Periods (CAV Test).....	4-15
Table 4-3 Crack Growth Results (Crack Growth Rates in inch/hour).....	4-16
Table 7-1 Load Case 1 Preload + Pressure = 0	7-10
Table 7-2 Load Case 2 Preload + Pressure = 1250 psi	7-11
Table 7-3 Load Case 3 Start-up Transient, Pressure = 1000 psi	7-12
Table 7-4 Load Case 4 Cooldown Transient, Pressure = 34.1 psi	7-13
Table 7-5 Steady State Stresses at Weld H-9.....	7-14
Table 7-6 Hydrotest Stresses at Weld H-9.....	7-15

List of Figures

<u>Figure</u>	<u>Page</u>
Figure 2-1. Overview of Vessel Nozzle and Attachment Weld Locations [2-2]	2-8
Figure 2-2. Steam Dryer Support Bracket Attachment Configuration.....	2-9
Figure 2-3. CBIN/CB&I Vessel Shroud Support Structure Attachment Configuration [2-2] ...	2-10
Figure 2-4. CE Vessel Shroud Support Structure Attachment Configuration (Jet Pump Plant)	2-11
Figure 2-5. CE Vessel Shroud Support Structure Attachment Configuration for Non-Jet Pump Plant [2-2].....	2-12
Figure 2-6. B&W Vessel Shroud Support Structure Attachment Configuration [2-2]	2-13
Figure 2-7. Instrumentation Nozzle Penetration Configuration [2-2].....	2-14
Figure 3-1. Intergranular Cracks in the Austenitic Cladding of the JPDR - Optical Micrograph of a Sectional Plane [3-5]	3-27
Figure 3-2. Transgranular Cracks in the Austenitic Cladding of the JPDR – Optical Micrograph of a Sectional Plane [3-5]	3-29
Figure 3-3. Pitting Corrosion at the Crack Tip in the Austenitic Cladding of the JPDR [3-5] ..	3-30
Figure 3-4. Pitting Corrosion at the Crack tip in the Austenitic Cladding of the JPDR [3-5] ...	3-31
Figure 3-5. Location of Cracks in Feedwater Nozzle - Cross Section [3-7]	3-33
Figure 3-6. Comparison of Observed and Calculated Crack Lengths [3-6].....	3-36
Figure 3-7. Old Safe End/Nozzle Configuration [3-10].....	3-37
Figure 3-8 Crack Profile - Chinshan 2 N2E Nozzle (Recirculation Inlet) [3-10]	3-39
Figure 3-9. Typical Location of Ultrasonic Inspection Indications in Nozzle/Safe-end Weldment at Brunswick Unit 1 before Weld Repair [3-10]	3-40
Figure 3-10. Typical Location of Ultrasonic Inspection Indications in Nozzle/Safe-end Weldment at Brunswick Unit 1 after Weld Repair [3-10]	3-41
Figure 3-11. Cracking in the Feedwater Piping of a BWR Adjacent to the RPV Nozzle [3-13]	3-42
Figure 3-12. Location of Cracks in Weld J of the Garigliano Steam Converter – Cross Section [3-7].....	3-44
Figure 3-13. Theoretical Crack Depth/Operating Time Relationships for the Garigliano Steam Converter [3-8].....	3-45
Figure 4-1. Crack propagation rate vs. stress intensity relationships in flowing water containing 200 ppb dissolved oxygen at 288°C (550°F) for constant load type specimens	4-17
Figure 4-2. Crack propagation rate vs. stress intensity relationships in flowing 288°C (550°F) water with 200 ppb dissolved oxygen for constant load type tests	4-18
Figure 4-3. Summary of Results of Round Robin Test: RPC102-4.....	4-19
Figure 4-4. Crack Growth of Low Alloy Steel: Four Phases of Loading in GENE Eight Specimen Test (1 cm/s = 1.4×10^3 in/h)	4-20
Figure 4-5. Summary of Results of Latter Phases of Eight Specimen Test for Trapezoidal Loading: RP C102-4.....	4-21
Figure 4-6. Crack length and conductivity as a function of time for reversing DC Specimen LAS 89	4-22
Figure 4-7. CAV crack growth rates plotted for each material and test period. The rates in periods 5, 6 and 7 are very low, nearing the resolution limit.	4-23

List of Figures (continued)

<u>Figure</u>	<u>Page</u>
Figure 4-8. Apparent crack growth rates determined by MPA-Stuttgart together with their chosen bounding line and the GE theoretical lines. Note that the bounding line at the lower K values is set by 1000 hr test time data.	4-24
Figure 5-1. BWRVIP Disposition Lines: Line for (a) Constant load and (b) Transient and Loading conditions shown.	5-10
Figure 6-1. Average Longitudinal and Transverse Residual Stress Distributions [6-8]	6-13
Figure 6-2. Longitudinal and Transverse Residual Stress Distributions [6-8].....	6-14
Figure 6-3. Longitudinal and Transverse Residual Stress Distributions [6-8].....	6-16
Figure 6-4. Longitudinal Through-Thickness Residual Stresses in Clad Plate Measured at Position 5.5 in. from Edge [6-9].....	6-16
Figure 6-5. Measured Residual Stress in Clad Plate	6-17
Figure 6-6. Residual Circumferential (Longitudinal Stress Due to Stress Relief PWHT from the Simulation of Two Layers of Clad [6-11] (Note 1 MPa = 0.145 ksi)	6-18
Figure 6-7. Variation of Clad Residual Stresses with Temperature.....	6-19
Figure 6-8. Proposed Clad Residual Stress Profile at Room Temperature	6-20
Figure 6-9. Photomacograph of Weld H9 at River Bend.....	6-21
Figure 6-10. Residual Stress through RPV Wall below H9 Weld	6-22
Figure 6-11. Stress Intensity Distribution Due to Clad Stress (Axial Flaw - $t_{clad}/t_{vessel} = 0.01$). ..	6-23
Figure 6-12. Stress Intensity Distribution Due to Clad Stress (Axial Flaw - $t_{clad}/t_{vessel} = 0.02$). ..	6-24
Figure 6-13. Stress Intensity Distribution Due to Clad Stress (Axial Flaw - $t_{clad}/t_{vessel} = 0.05$). ..	6-25
Figure 6-14. Stress Intensity Variation for Various Clad to Vessel Thicknesses (Axial Flaw). ..	6-26
Figure 6-15. Through-wall Stress Intensity Factor Distribution for Vessel Weld Residual Stress (Axial Flaw).....	6-27
Figure 6-16. Through-wall Stress Intensity Factor Distribution in a Vessel with Membrane Stress of 10 ksi (Axial Flaw with Aspect Ratio of 0.1 and 0.5).....	6-28
Figure 6-17. Through-wall Stress Intensity Factor Distribution in a Vessel with Bending Stress of 10 ksi (Axial Flaw with Aspect Ratio of 0.1 and 0.5).....	6-29
Figure 6-18. Cracked Cylinder to Edge-Cracked Plate K_I Curvature Correction Factor for Circumferential Flaws in a Vessel ($t/R = 0.1$).....	6-30
Figure 6-19. Stress Intensity Distribution Due to Clad Stress (Circumferential Flaw - $t_{clad}/t_{vessel} = 0.01$).....	6-31
Figure 6-20. Stress Intensity Distribution Due to Clad Stress (Circumferential Flaw - $t_{clad}/t_{vessel} = 0.02$).....	6-32
Figure 6-21. Stress Intensity Distribution Due to Clad Stress (Circumferential Flaw - $t_{clad}/t_{vessel} = 0.05$).....	6-33
Figure 6-22. Stress Intensity for Various Clad to Vessel Thicknesses (Circumferential Flaw) ..	6-34
Figure 6-23. Through-wall Stress Intensity Factor Distribution for Vessel Weld Residual Stress (Circumferential Flaw)	6-35
Figure 6-24. Through-wall Stress Intensity Factor Distribution in a Vessel with Membrane Stress of 10 ksi (Circumferential Flaw)	6-36
Figure 6-25. Through-wall Stress Intensity Factor Distribution in a Vessel with Bending Stress of 10 ksi (Circumferential Flaw)	6-37

List of Figures (concluded)

<u>Figure</u>	<u>Page</u>
Figure 6-26. Parameter F_t to Describe Stress Intensity Factor K_I for the Part-Through-Wall, Part Circumference Flaws [15]	6-38
Figure 6-27. Flaw Reduction Factors for Determination of K_I for Weld Residual Stresses in BWR Shrouds with Part-Circumference Flaws	6-39
Figure 7-1. Reactor Vessel Head and Flange.....	7-16
Figure 7-2. Vessel Head Stress Distribution	7-17
Figure 7-3. Allowable Flaw Size Determination for Vessel Head (360° Flaw)	7-18
Figure 7-4. Stress Corrosion Cracking Evaluation Results (Circumferential Flaw) for Vessel Head Evaluation Results	7-19
Figure 7-5. Configuration of Vessel at Weld H9 (Shroud Support Plate to Vessel).....	7-20
Figure 7-6. Details of Vessel Configuration at Weld H9.....	7-21
Figure 7-7. Allowable Flaw Size Determination for Vessel Near Weld H-9 (360° Flaw)	7-22
Figure 7-8. Stress Corrosion Cracking Evaluation Results for Vessel Near Weld H-9 (Circumferential Flaw).....	7-23
Figure 7-9. Allowable Flaw Size Determination for Vessel Head (Axial Flaw)	7-24
Figure 7-10. Stress Corrosion Crack Growth for Vessel Head and Comparison to Allowable (Axial Flaw).....	7-25
Figure 7-11. Allowable Flaw Size Determination for Vessel Weld Near H-9 (Axial Flaw)	7-26
Figure 7-12. Stress Corrosion Crack Growth for Vessel Weld New Weld H-9 (Axial Flaw)...	7-27

Executive Summary

The purpose of this report is to provide a methodology for assessment of stress corrosion crack growth of low alloy steel (LAS) reactor pressure vessel (RPV) components in the boiling water reactor (BWR) environment.

Low alloy steel alloys are used in the fabrication of RPVs and associated nozzles. These materials generally have a combination of high strength and excellent fracture toughness properties that make them suitable for design of the vessels at operating conditions. For BWR vessels designed using the 1965 Edition of ASME Code, Section III; ASTM A-302, Grade B material was used for the fabrication of the vessel. For vessels designed using subsequent editions of the Code, SA-533, Grade B, Class 1 LAS plate material was used. The associated forging material used in nozzles is typically SA-508, Class 2. These materials are usually clad with austenitic stainless steel weld metal, typically Type 308 stainless steel, to provide improved general corrosion or pitting resistance during low temperature shutdown as well as to allow for welding of attachments without the requirement for post weld heat treatment (PWHT).

Various vessel attachment types and structure configurations that are encountered in the BWR industry are discussed in Section 2 of this report. Examination of the materials of the attachment welds indicate that some of them are fabricated from Alloy 182 weld metal which has been shown to be susceptible to intergranular stress corrosion cracking (IGSCC). Recent findings at two BWR plants also demonstrated that under special circumstances, cracking can occur in the stainless steel cladding, especially in areas where manual welding is performed. Any initiated crack could propagate by SCC to the LAS RPV. The crack growth of stainless steel and the Alloy 182 weld material has been addressed previously in separate BWRVIP reports, (BWRVIP-14 and BWRVIP-59).

While the field experience with these LAS vessel plate and nozzle materials in the BWR environment has been excellent, there have been a limited number of incidents where cracking has initiated in weldments attached to nozzle butter, or where vessel cladding cracks have come

into contact with the underlying vessel materials. No incidents of significant propagation of the cracks in LAS through SCC have been reported. Yet, there is a concern that environmentally assisted cracking (EAC), either fatigue or stress corrosion related, may propagate within these materials thereby affecting the structural integrity of the components. The current status of global operating experience with RPVs in BWRs with regard to EAC in general and SCC in particular is presented in Section 3. Specific conclusions have been drawn from the individual cases reported.

Section 4 is a review of the current state of understanding SCC in LASs based on data from laboratory size test specimens. Experimental studies performed under the auspices of EPRI and GE have shown that, indeed, low alloy pressure vessel steels may be susceptible to SCC at high stress intensities, depending on the environment, load transient and material conditions. Laboratory testing as well as confirmatory reactor site testing results are presented. The summary of all the data i.e., field experience, as well as laboratory test result, in the context of its relevance to crack growth modeling and disposition curves, reveals that there are a large number of variables that can affect cracking behavior, many of which were not always adequately controlled during the testing.

In Section 5 various crack growth theories that are discussed relate crack propagation to oxidation at the crack tip and the stress/strain conditions at the crack tip.

Content Deleted - EPRI Proprietary Information

Currently there are three possible crack propagation rate vs. stress intensity disposition relationships that might be proposed for LASs in high temperature water. Two which have some fundamental understanding to support their formulation, are:

Content Deleted - EPRI Proprietary Information

Section 6 describes the residual stress distributions for vessel cladding and the vessel attachment welds. Experimental and analytical weld and clad residual stresses are presented for these locations. Stresses associated with BWR attachment welds are classified into fabrication and operational stresses. Fabrication stresses consist of weld residual stresses resulting from welding the vessel plates, clad stresses due to the application of the clad and subsequent post weld heat treatment, and the stresses resulting from the attachment weld. Operational stresses are those associated with the normal operation of the plant and consist of stresses analyzed in the ASME Code stress reports.

Also presented in Section 6 are the fracture mechanics models used to determine the through-wall stress intensity factor (K) distributions for the through-wall stress profiles for the clad and the attachment weld residual stress profiles. K distributions were also derived for operational

stresses which consist of membrane and bending stresses. The allowable flaw sizes were also discussed in this section. The determination of the allowable flaw sizes is based on the methodology provided in ASME Section XI, IWB-3600.

Section 7 presents two examples illustrating the use of this methodology to evaluate crack propagation through SCC in the LAS RPV material. The examples presented are for the top head flange and for the shroud support plate. In both cases, through clad cracks are assumed as the initial condition and a crack growth evaluation is performed into the vessel wall. The evaluations were performed considering both circumferential and axial flaws.

**Content Deleted -
EPRI Proprietary Information**

The BWRVIP proposes that the methodology presented in this report including the crack growth disposition curves be used as a basis for evaluation of stress corrosion crack growth in LAS RPVs.

CONVERSION FACTORS

In this report, attempt has been made to provide both SI and English units. Occasionally, only English units are provided.

To convert from	to	multiply by
ksi	MPa	6.895
ksi $\sqrt{\text{in}}$	MPa $\sqrt{\text{m}}$	1.100

1.0 INTRODUCTION

LAS alloys are used in thick section pressure vessel plate and vessel nozzle applications where a combination of high strength, excellent fracture toughness are required and excellent SCC resistance. For the BWR, the typical plate material is SA533 Gr. B and the typical nozzle material is SA508 Cl 2. These materials are usually clad with austenitic stainless steel weld metal, typically Type 308 stainless steel to provide improved general corrosion or pitting resistance during shutdown as well as to allow for welding of attachments without the requirement for PWHT. However, the excellent performance of these materials in BWR services has allowed for the use of some unclad nozzles in more recent plants. Whereas, the field experience with these LAS vessel plate and nozzle materials has been excellent in BWR service, there have been a limited number of incidents where cracking that has initiated in weldments attached to nozzle butter or where vessel cladding cracks have come into contact with the underlying vessel materials. Although no incidents where significant propagation of the cracks in the LAS have been reported under constant load, there is a concern that EAC may occur within these materials, thereby affecting the structural integrity of the components.

Several studies have been performed examining the SCC susceptibility of LAS pressure vessel materials in the oxidizing BWR environment. These studies described in Sections 4 and 5 of this report have included modeling and experimental studies examining both the crack initiation and crack growth behavior of these alloys in the BWR environment. Also included have been evaluations of the effects of vessel attachment welds on the SCC growth into the RPV. These studies have demonstrated that the resistance for SCC propagation is good and that crack growth in the LAS vessel material under constant load usually occurs only at very high stress intensities.

Extensive research has also been performed on these steels examining the fatigue crack initiation and propagation behavior in light water reactors. These data have demonstrated that under cyclic loading conditions at sufficient stress amplitudes, fatigue can produce significant crack propagation in these alloys in the BWR environment. Growth rates are also accelerated by the corrosive behavior of the environment. However, for the LAS components in the BWR, the only

significant fatigue contributions occur in nozzles where injection of colder feedwater water is allowed to impinge on nozzles operating at reactor operating temperatures. Recent design changes in the feedwater and CRD return nozzles have reduced the likelihood of this event.

The objective of this study is to provide a methodology for determining the stress corrosion cracking crack growth rate of low alloy steel reactor pressure vessel components in the BWR environment. Section 2 of this report describes the RPV configurations and vessel attachment.

Section 3 describes the plant operating experience for LAS components. Section 4 presents the laboratory SCC studies providing industry information on the BWR SCC response of LAS.

Section 5 presents the crack growth rate/stress intensity disposition relationships developed for LAS in BWR water. Operational and residual stress determination for vessel attachments and vessel cladding and the resultant stress intensities as a function of crack depth are presented in Section 6. Section 7 presents the fracture mechanics methodology for the vessel providing examples of the crack growth methodology applied to attachments or to the RPV clad. Section 8 presents the report summary, conclusions and recommendations.

2.0 RPV CONFIGURATIONS AND VESSEL ATTACHMENT TYPES AND LOCATIONS

2.1 BWR Vessel Configurations

A BWR pressure vessel consists of a cylinder welded to a hemispherical bottom head. It is welded to the flange with bolt holes such that it can be bolted to a removable hemispherical top head with a mating flange at the top. An excellent description of the material and fabrication process for BWR RPVs is provided in References 2-1, 2-2, BWRVIP 05 and 48 (2-3 and 2-4). Table 2-1 taken from Reference 2-1 shows that for BWR vessels designed using the 1965 Edition of ASME Code, Section III; ASTM A-302, Grade B material, was used for the fabrication of the vessel. For vessels designed using subsequent editions of the Code, SA-533, Grade B, Class 1 LAS plate material was used. The associated forging material is typically SA-508, Class 2. Several plates are used to fabricate both the cylindrical and hemispherical portions typically using the submerged metal arc welding process. Welding of these plates in both the longitudinal and circumferential directions result in some weld residual stresses in the vicinity of the welds. As shown in Table 2-2, the ratio of the vessel shell thickness to the inside radius is fairly constant (approximately 0.04-0.05) for most BWRs except for two early BWRs (Oyster Creek 1 and Nine Mile Point 1), which are relatively thicker.

The RPV is clad on the inside surface to increase its resistance to general corrosion at low temperatures. The cladding was almost exclusively performed using Type 308/309 stainless steel weld metal and using the arc welding process. The applications of the cladding in most cases were performed using the submerged arc welding process (SAW), especially for the later plants. The manual shielded metal arc welding process (SMAW) was used in areas that were not amenable to the SAW process as in the dollar plate region of the top head and for most weld repairs. Most of the clad surface of BWR vessels is in the "as-clad" condition, except in areas where machining was specified to meet fabrication tolerances and non-destructive examination (NDE) requirement such as flange mating surfaces. In the "as-clad" condition, there was no specific surface treatment of the clad surface. The thickness of the cladding can vary from 3.175

to 5.563 mm (0.125 to 0.219 inches), as shown in Table 2-1, for few typical BWRs. The clad thickness-to-vessel thickness ratio for all BWRs is expected to vary between 0.01 and 0.05 as demonstrated for the typical cases in Table 2-2.

On many areas of the vessel, additional support structures were provided by welding brackets and other attachments to the vessel (2-2 and 2-3). The attachment welds for these structures, in general, were not directly welded to the cladding since the cladding was not qualified as a structural weld. This was especially true for the earlier vintage plants, where weld build-ups or pads were applied directly to the RPV base material so that the attachment welds could be welded on these pads. Grooves were either left at the locations for the attachment weld during manual welding or removed by machining if automatic deposition techniques were used for the purpose of applying the weld build-up. For more recent plants, where the cladding was qualified as a structural weld material, the build-ups are applied directly to the cladding before the attachment weld is made. A summary of attachment welds for a typical BWR is presented in Table 2-3. As can be seen from Figure 2-1, most attachment welds are removed from the active core region, therefore, neutron embrittlement is not an issue in the evaluation of most BWR attachment welds.

The ASME Code [2-5] requires that PWHT be applied to RPVs following welding operations (both cladding and weld build-ups) to reduce residual stresses arising from the welding and to temper any transformed martensite in the low alloy steel vessel. As required by the ASME Code, PWHT was usually performed at a temperature of 1100-1200°F for 12 to 48 hours. Subsequent PWHT of structures attached to the austenitic material weld build-ups that have previously received PWHT is not required. As will be shown later, PWHT may not completely eliminate the residual stresses in the cladding, weld build-ups and even the shell welds of the vessel. It is believed that these residual stresses may have played a major role in the cracking problems that have been observed to date in BWR attachment welds and cladding.

2.2 Classification of Attachment Welds

The attachment welds listed in Reference 2-2 can be classified into three broad categories:

- The first group consists of butt welds joining the RPV nozzle to pipe or safe-end components. This group basically consists of pipe-to-pipe welds on the outside of the RPV and as such does not fit into the description of classical attachment welds inside the RPV. This group, therefore, will not be considered as vessel attachment welds in this report.
- The second group consists of plate materials welded to the inside surface of the RPV. This group consists of attachment welds of most brackets attached to the RPV such as the steam dryer bracket, feedwater sparger bracket, etc. The designs of these brackets differ depending on the vessel fabrication vendor as illustrated in Figure 2-2 for the steam dryer bracket. This figure illustrates that the material of the bracket is usually Type 304 stainless steel and the attachment weld is either E308/308L or Alloy 182 (ENiCrFe-3). The weld can be attached directly on the stainless steel clad or onto a pad welded to the RPV after machining a groove in the RPV. A subsection of this group consists of shroud support plate vessel attachment welds shown in Figures 2-3 through 2-6. Notice that the material of the attachment welds consist mainly of Alloy 600 (SB-168) and the attachment welds are also fabricated using nickel base weld metal.
- The third group consists of nozzle penetration welds welded directly to the RPV. This group consists of the control rod drive penetration, in-core housing penetrations, instrumentation nozzles, core differential pressure and liquid control penetrations. Typical configuration of the attachment welds in this group is illustrated by the control rod drive penetration configuration in Figure 2-7.

Examination of the materials of the attachment welds shown in Figures 2-1 through 2-7 indicate that some of them are fabricated from Alloy 182 weld metal which has been shown to be

susceptible to IGSCC. Recent findings at two BWR plants also demonstrated that cracking may occur in the stainless steel cladding, especially in areas where manual welding is performed. Cracks in these attachment welds can propagate through a combination of SCC and fatigue to the LAS RPV. Although the LAS is highly resistant to SCC, isolated incidents of SCC propagation into the RPV have been reported raising questions about its susceptibility to SCC. Experimental studies performed under the auspices of EPRI and GE have shown that, indeed, low alloy pressure vessel steels are susceptible to SCC, under severe oxidizing, loading and material heat treatment conditions.

2.3 References

- 2-1. ASME Code, Section XI Working Group on Operating Plant Criteria, "White Paper on Reactor Vessel Integrity Requirements for Level A and B Conditions," EPRI TR-100251, January 1993.
- 2-2. K. S. Brown, R. C. Szombathy, and H. S. Mehta, "Reactor Vessel Attachment Welds: Degradation Assessment," EPRI Report No. NP-7139-D, Palo Alto, CA, May 1991.
- 2-3. "BWR Reactor Pressure Vessel Shell Weld Inspection Recommendations (BWRVIP-05)," EPRI TR-105697, Palo Alto, CA, September 1995.
- 2-4. "Vessel ID Attachment Weld Inspections and Flaw Evaluation Guidelines (BWRVIP-048)," EPRI TR-108724, Palo Alto, CA, February 1998.
- 2-5. ASME Boiler and Pressure Vessel Code, Section XI, 1992 Edition.

Table 2-1

Design Information for GE Nuclear Energy Reactor Vessels [2-1]

**Content Deleted -
EPRI Proprietary Information**

Table 2-2
Clad to Thickness Ratios for Typical Reactor Vessels [2-2]

**Content Deleted -
EPRI Proprietary Information**

Table 2-3
Summary of Attachment Welds [2-2]

- Top head nozzles (vent, head spray and spare)
- Steam dryer hold down brackets
- Steam outlet nozzles
- Steam dryer support brackets
- Guide rod brackets
- Instrumentation nozzles
- Feedwater nozzles
- Feedwater sparger brackets
- Core spray nozzles
- Core spray pipe brackets
- Control rod drive hydraulic system return nozzles
- Jet pump riser brackets
- Surveillance specimen capsule holder brackets
- Recirculation inlet nozzles
- Recirculation outlet nozzles
- Jet pump instrument nozzles
- Shroud support structure
- Core differential pressure and liquid control penetrations
- Control rod drive penetrations
- In-core housing penetrations
- Drain nozzles

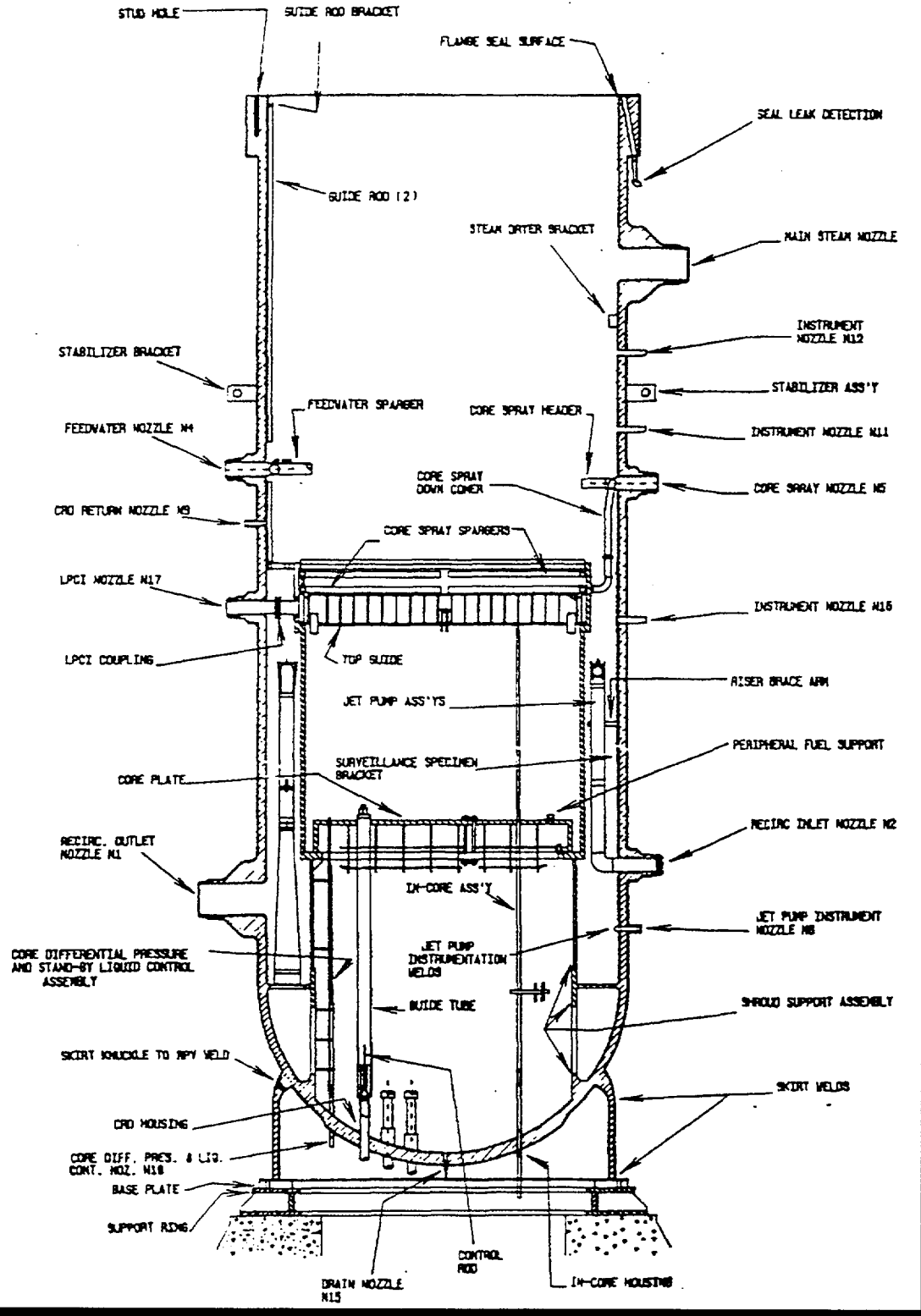


Figure 2-1. Overview of Vessel Nozzle and Attachment Weld Locations [2-2]

**Content Deleted -
EPRI Proprietary Information**

Figure 2-2. Steam Dryer Support Bracket Attachment Configuration

**Content Deleted -
EPRI Proprietary Information**

Figure 2-3. CBIN/CB&I Vessel Shroud Support Structure Attachment Configuration [2-2]

**Content Deleted -
EPRI Proprietary Information**

Figure 2-4. CE Vessel Shroud Support Structure Attachment Configuration (Jet Pump Plant)
[2-2]

**Content Deleted -
EPRI Proprietary Information**

Figure 2-5. CE Vessel Shroud Support Structure Attachment Configuration for
Non-Jet Pump Plant [2-2]

**Content Deleted -
EPRI Proprietary Information**

Figure 2-6. B&W Vessel Shroud Support Structure Attachment Configuration [2-2]

**Content Deleted -
EPRI Proprietary Information**

Figure 2-7. Instrumentation Nozzle Penetration Configuration [2-2]

3.0 OPERATING EXPERIENCE WITH PRESSURE VESSELS IN BWR PLANTS RELATED TO ENVIRONMENTALLY ASSISTED CRACKING WITH PARTICULAR EMPHASIS ON STRESS CORROSION CRACKING *

3.1 Introduction

The status of global operating experience with BWR RPVs with regard to EAC in general and SCC in particular is presented in this report as a contribution to an ongoing evaluation of this and related topics by the EPRI PEER group. It contains a summary of all the known damage to date in BWR pressure vessels worldwide that may be related to EAC, with particular emphasis on SCC.

In the past, (e. g., in connection with findings from nondestructive examination (NDE) of RPV heads in BWRs in the USA [3-1]), questions have arisen regarding the long-term integrity of the RPVs in BWR plants, in particular with regard to potential susceptibility of the austenitic cladding or the LAS base material to SCC during continuous operation. Only a few, individual cases of incipient cracking in the RPV during operation are known and these are described below. This section of the report also contains a brief summary of SCC-induced damage in another pressure vessel (steam converter) of an Italian BWR.

First, it should be noted that no RPV damage due to SCC, i. e., at constant load, during steady-state operation, is known in pressurized water reactors (PWR) worldwide. Cases of damage to the steam generators of various PWRs (particularly cladding cracks in the primary channel head, as well as secondary-side crack development in the SG shells in some plants such as Indian Point, Surry and Zion) are not covered in this report, since the results cannot be directly transferred to BWR plants, (e. g., due to such factors as the different water chemistry). Details concerning the latter events are reported in Reference 2-2.

* This section was prepared by Armin Roth (Siemens) and John Hickling (CMC) and includes input by reviewers.

3.2 Research Reactors

3.2.1 *Elk River, USA*

- 22 MWe, 1st criticality 1962

A circumferentially oriented network of fine cracks in the Type 308L stainless steel RPV cladding was detected in 1961, before nuclear commissioning of the Elk River plant. These were initially attributed to hot cracking during manufacturing. However, one year later, extensive cracks were discovered in the steam plenum just below the RPV flange. These had apparently occurred due to IGSCC during operation. The cladding process itself is regarded as the main reason for the damage, since a dilution of the high-alloy, austenitic cladding with the low-alloy steel base material (A 212B) had occurred, resulting in the formation of martensite in the stainless steel weld material [3-3, 3-4]. The maximum crack depth was approximately 5 mm (0.2 in.) and cracks did not reach the LAS base material of the RPV at any location.

3.2.2 *Argonne EBWR, USA,*

- 5 MWe, 1st criticality 1956

Numerous cladding cracks were detected in the RPV of the EBWR plant in an inspection in 1965 after approximately six years of operation, but only in areas in which cladding had been performed by spot-welding Type 304 stainless steel plates to the LAS base material (A 212B). There were no indications in the conventional weld clad areas of the RPV. The primarily intergranular cracks in the highly sensitized austenitic stainless steel weld cladding were initially attributed exclusively to thermally-induced, mechanical overload fracture during manufacturing [3-3]. However, a contribution from SCC was later considered to be probable [3-4].

The cracks appeared primarily in the steam plenum of the EBWR RPV and penetrated the cladding at several locations over a total length of approximately 12 m (472 inches). However, extensive investigations, including removal of boat samples, revealed neither crack propagation

in the base material nor pronounced pitting corrosion at the interface between the austenitic and ferritic materials.

No repair of the ground-out cladding areas was performed before further operation of the EBWR, with the result that a total of approximately 0.09 m² (140 in²) of the LAS was directly exposed to the reactor water. The program initiated for monitoring these locations apparently did not yield any indications, hence degradation of RPV integrity by EAC did not occur.

3.2.3 JPDR, Tokai, Japan

- 10 MWe, operating period 1963 –1976

3.2.3.1 Type and Extent of Damage

In 1966, after approximately 13,000 hours of operation, extensive cracking was detected at several locations on the inside of the RPV head as well as, to a much lesser extent, in the cylindrical section and in the bottom dished head [3-5]. These cracks appeared primarily at locations where all three layers of the austenitic cladding had been manually welded. The remaining cladding areas of the same material (1st layer: manual weld with Type 309Mo stainless steel 2nd and 3rd layers: automatic weld with Type 308L stainless steel) were free of cracks.

The predominantly intergranular cracks near the cladding surface (Figure 3-1) were attributed to ferrite-free areas of the austenitic matrix with coarse dendrite formation. Adjacent areas without cracking exhibited a standard weld metal structure with several percent delta ferrite. With increasing depth in the cladding, the branched cracks also followed transgranular paths (Figure 3-2) and appeared to be related to martensite formation in the first cladding layer near the transition to the base material.

Many of the cracks extended to the LAS base material (A 302 B), but no further crack propagation was detected in the LAS. There was much more extensive pitting at or along the phase boundary between the austenitic cladding and the LAS base material with differing corrosion resistance (Figure 3-3), where a possible spatial orientation of the localized corrosion attack to the existing stresses (Figure 3-4) was not ruled out [3-5].

3.2.3.2 Cause and Mechanism of Damage

The cracks in the cladding are considered to be caused by incorrect composition of the manually welded areas (including chromium depletion and carburization) due to excessive mixing of the layers or reaction of the first layer with the base material. Thus, this was clearly a case of manufacturing defects.

The Japanese authors [3-5] identified SCC in the austenitic stainless steel as the exclusive damage mechanism, resulting from a microstructure with impaired corrosion resistance together with the oxygen content in the steam condensate typical for BWRs and possible impurities from the reactor water.

**Content Deleted -
EPRI Proprietary Information**

3.2.3.3 Derivable Crack Propagation Rate

**Content Deleted -
EPRI Proprietary Information**

**Content Deleted -
EPRI Proprietary Information**

3.2.3.4 Remedial Action

The visible defects in the RPV head were ground out and the cladding was repaired by welding at these points. However, a small number of cracks were left for further monitoring. The places at which boat samples had been removed were subjected only to slight grinding. This left local hollows in the cladding down to the base material. A complementary test program proved that no additional risk due to pitting or galvanic corrosion was to be anticipated at such locations.

3.2.3.5 Relevance for Assessment of SCC in other BWR Plants

**Content Deleted -
EPRI Proprietary Information**

3.3 BWRs in Commercial Operation

3.3.1 Feedwater Nozzle Cracking in US Design BWRs

- Millstone 1, 660 Mwe, Operating Period 1970 – 1998

The most important case of damage was detected in 1974 first at Millstone 1, and subsequently at approximately 17 additional plants in the USA up to 1978. It should be noted that the feedwater nozzle cracking was due to corrosion fatigue. Crack initiation and growth were demonstrated using fatigue analysis. Subsequent repair that eliminated the thermal fatigue cycle has been successful. No explicit SCC role was identified.

3.3.1.1 Type and Extent of Damage

As an example, the damage in Millstone 1 was originally detected during nondestructive examination of cracked areas of the austenitic feedwater sparger, as the adjacent cladding at the inner bore radius of the actual feedwater nozzles was also subjected to dye-penetrant examination. Following recognition of the non-plant-specific nature of the problem, extensive testing determined that cracks had developed both at the nozzle radius (to a maximum depth of approximately 18 mm [0.7 inches]) as well as in the cylindrical section of the feedwater nozzle bore (up to a maximum depth of approximately 38 mm [1.5 inches]) in several plants [3-6].

3.3.1.2 Cause and Mechanism of Damage

On the basis of metallographic and fractographic investigations of boat samples, it was determined that the mainly transgranular cracking in the Type 308 stainless steel cladding and in the A508 LAS base material was primarily due to fatigue [3-7].

Extensive stress analysis further led to the conclusion that two different fatigue mechanisms were involved: high-cycle thermal fatigue (frequencies of 0.1 to 1 Hz) during crack initiation and growth through the cladding (i. e. up to a depth of approximately 6 mm [0.24 inches]) and low-cycle corrosion fatigue due to the BWR reactor water environment (including the effects of cycling at very low frequency) during further crack propagation in the base material. A possible contribution from SCC to crack propagation is conceivable, but the general agreement between

crack depth and number of plant transients points to a predominant influence of the cyclic loading.

3.3.1.3 Derivable Crack Propagation Rate

In the plants with the most unfavorable conditions in the area of the feedwater nozzles, the original cracking due to thermal fatigue apparently occurred within months.

Further crack growth in the low alloy steel base material of the nozzle area was initially explained by loading due to plant transients (primarily startup and shutdown, but also reactor trip and turbine trip) [3-6]. The affected plants exhibited roughly 40 to 120 such transients (Figure 3-6). Further analysis of the influence of such cyclic loading assigned a greater significance to loads associated with steady-state conditions [3-8] or to a lower number of main transients [3-9].

**Content Deleted -
EPRI Proprietary Information**

3.3.1.4 Remedial Action

Various medium-term and long-term remedial measures were initiated to prevent the aforementioned problems re-occurring in the feedwater nozzle:

- Replacement of the thermal sleeve with an improved design which also ruled out the possibility of bypass leakage flow.
- Introduction of “protective” plant operating procedures to reduce thermal loads.

- Grinding out of cladding on the bore radius of the nozzle (in at least 5 plants) or installation of unclad nozzles (from the BWR 4 and BWR 5 series onwards).

The latter measure, in particular, was subjected to extensive theoretical and experimental investigation. Significant advantages are as follows:

- Reduction of cyclic thermal loading by a factor of approximately two due to elimination of differing thermal material properties.
- Improvement in ultrasonic examinability in the nozzle area by a factor of at least four (bore radius) or five (cylindrical section).
- Reduction of any possible risk of incipient cracking due to SCC in areas of lower cladding quality.
- Elimination of any cracks present in the base material.

In 1978, a corrosion assessment of this measure considered degradation of the integrity of the RPV wall from SCC to be unlikely, although few data on the corrosion behavior of the LAS A 508 were available at that time [3-6]. Potential increased susceptibility to uniform corrosion and/or pitting corrosion was considered, but was categorized as insignificant owing to the positive operating experience with already existing unclad surfaces (nozzle/piping transition area and repair locations on nozzles).

3.3.1.5 Relevance for Assessment of SCC in other BWR Plants

**Content Deleted -
EPRI Proprietary Information**

Content Deleted - EPRI Proprietary Information

3.3.2 Inlet nozzle safe end cracking (Alloy 182 cladding)

- Examples: Chinshan 1 and 2, GE BWR (604 MWe), initial startup 1977 and 1978, respectively.

3.3.2.1 Type and Extent of Damage

Extensive cracking was detected in Chinshan 1 and Chinshan 2 in 1986 and 1987, respectively, the area of the welds between the inlet nozzle and safe end of the recirculation loop [3-10]. The cracking was limited primarily to the Alloy 182 butter area and the associated transition between Alloy 182 and the austenitic stainless steel nozzle cladding (Figure 3-8). However, in one case, limited crack propagation (maximum depth approximately 7 mm [0.27 in], based upon measurements during grinding) was also detected in the A508 LAS nozzle material [3-11].

Crack initiation is assumed to have occurred in the safe end itself on the basis of a similar finding made earlier in the Pilgrim plant [3-10, 3-12].

3.3.2.2 Cause and Mechanism of Damage

The damage is assumed to be caused by high residual stresses in the weld area together with the use of a material of limited SCC resistance. Extensive laboratory investigations show that manual welds made with a covered Alloy 182 electrode exhibit significantly worse SCC behavior than welds made with high-chromium Alloy 82 filler wire.

No conclusions can be drawn regarding the single defect in the LAS as it was simply ground out without any metallurgical investigation.

3.3.2.3 Derivable Crack Propagation Rate

The available data do not permit the crack propagation rate to be determined.

3.3.2.4 Remedial Action

Temporary repairs were first performed by weld overlaying on the outside of the nozzle. With the exception of the crack extending into the base material, which was ground out and repaired by welding, essentially only the Alloy 182 areas exposed to the reactor water environment were later protected against renewed SCC by weld overlaying with Alloy 82 to form a corrosion resistant cladding.

3.3.2.5 Relevance for Assessment of SCC in other BWR Plants

**Content Deleted -
EPRI Proprietary Information**

3.3.3 Inlet nozzle cracking (Alloy 182 cladding)

- Brunswick 1, GE BWR 4 (821 MWe), initial startup 1976

Significant damage to the comparable nozzle/safe end welds as in the Chinshan plant was assumed on the basis of extensive NDE findings in the Brunswick 1 plant (Figure 3-9), but with the main difference that the incipient crack was in the area of the actual nozzle, although still within the region clad with Alloy 182 [3-10]. The ultrasonic inspection data (Table 3-1) initially

indicated defects associated with the LAS Alloy 182 interface. However, after an external weld repair (Figure 3-10), there were so many changes in the NDE indications (apparent increase and decrease in the number of cracks, shifting of crack fields, etc.) that these may have been false indications due to the complex inspection geometry. The plant was returned to operation until complete nozzle replacement in the fall of 1990.

3.3.4 EAC in the Feedwater Pipe to Nozzle Weld of a non-US Design BWR

Relatively deep cracks were detected by NDE in unclad regions at the feedwater nozzles of a German BWR (800 MWe, initial startup 1976) after about 7000 hours of operation.

3.3.4.1 Type and Extent of Damage

In contrast to the nozzle cracking experienced in GE BWR plants, the prime damage location was on the feedwater side in the pipe to nozzle weld. Major circumferential cracks had originated in the 12 o'clock position of the horizontal piping at weld-root defects and had propagated up to a maximum depth of 95 % of the wall thickness (8.8 mm [0.35 inches]). Secondary damage was also observed in the form of numerous minor cracks of maximum depth 0.8 mm [0.031 inches], predominantly in the 6 o'clock position of the ferritic base metal of the feedwater pipe and the nozzle, as well as in the weld itself.

3.3.4.2 Cause and Mechanism of Damage

On the basis of extensive metallographic and fractographic examinations [3-13], it was determined that both deep and minor cracking were due to EAC. Temperature and strain measurements, performed on a parallel feedwater line, revealed that the piping adjacent to the feedwater nozzles was subjected to severe thermal loading during certain phases of reactor operation, (e.g., hot standby). Both rapid thermal shocks (with strain rates of the order of 10^{-3} /s) and slower strain transients (10^{-5} /s to 10^{-7} /s) resulting from thermal stratification were observed

The latter produces a practically homogeneous strain distribution throughout the pipe wall and may have been more important during crack growth, since the strain rates lie in the critical region for so-called strain-induced corrosion cracking (SICC) of ferritic materials [3-14]. The ultimate location and distribution of the cracks was determined by the weld geometry and by bending due to constrained thermal displacement of the piping.

3.3.4.3 Derivable Crack Propagation Rate

**Content Deleted -
EPRI Proprietary Information**

3.3.4.4 Remedial Action

In terms of the mechanical loading, certain operational situations, (e. g. hot standby at low feedwater flow), are no longer permitted and transient loading has also been reduced by the avoidance, where possible, of temperature gradients. Freedom from weld defects in the replacement, thicker-walled piping has also undoubtedly contributed to the prevention of renewed crack initiation at the above location.

3.3.4.5 Relevance for Assessment of EAC in other BWR Plants

**Content Deleted -
EPRI Proprietary Information**

3.3.5 Reactor vessel head cracking (heads clad with austenitic stainless steel)

3.3.5.1 Quad Cities 2 Plant GE BWR 3 (789 MWe), initial startup 1972

3.3.5.1.1 Type and Extent of Damage

During the annual refueling outage of Quad Cities 2 [3-1] in March 1990, defects (stain patches) were visually detected at various points on the RPV head cladding (approximately 940 mm [37 inches] above the edge of the vessel head flange).

**Content Deleted -
EPRI Proprietary Information**

**Content Deleted -
EPRI Proprietary Information**

3.3.5.1.2 Cause and Mechanism of Damage

**Content Deleted -
EPRI Proprietary Information**

3.3.5.1.3 Derivable Crack Propagation Rate

**Content Deleted -
EPRI Proprietary Information**

3.3.5.1.4 Remedial Action

Initially, most of the cracks were simply ground out without subsequent welding repair, so the plant was operated for an additional cycle with local hollows extending to the base material. In addition, some cracks were deliberately left untreated to monitor their behavior during further operation. A detailed fracture-mechanics analysis indicated no threat to RPV integrity, even under consideration of possible EAC crack growth.

Subsequent re-inspection of the cracks which had not been ground out gave no indication of further growth.

3.3.5.1.5 Relevance for Assessment of SCC in other BWR Plants

**Content Deleted -
EPRI Proprietary Information**

3.3.5.2 *Vermont Yankee*

3.3.5.2.1 Type and Extent of Damage

In Vermont Yankee [3-1], rust patches were observed on the stainless steel cladding of the vessel head during an inspection in 1992. The inspection conducted to address concerns for cracking similar to that observed in the clad vessel head at Quad Cities Unit 2 as identified in the GE Service Information Letter No. 539.

**Content Deleted -
EPRI Proprietary Information**

**Content Deleted -
EPRI Proprietary Information**

3.3.5.2.2 Cause and Mechanism of Damage

**Content Deleted -
EPRI Proprietary Information**

3.3.5.2.3 Derivable Crack Propagation Rate

No values were derived for the propagation rate of the cladding cracks, many of which may have been present in the head for some considerable time before detection.

3.3.5.2.4 Remedial Action

A detailed fracture-mechanics analysis indicated no threat to RPV integrity, even under consideration of hypothetical SCC crack growth in the ferritic base material. Thus no repairs were required, although re-inspection of the head flange cladding was planned.

3.3.5.2.5 Relevance for Assessment of SCC in other BWR plants

Content Deleted - EPRI Proprietary Information

3.3.6 Reactor vessel head cracking (*unclad head*)

James A. FitzPatrick Plant GE BWR (816 MWe), initial startup 1975

Four defects were detected in the upper circumferential weld of the unclad RPV head during routine ultrasonic testing during the annual refueling outage in 1990.

Content Deleted - EPRI Proprietary Information

Following a fracture-mechanics evaluation, the licensing authority approved plant restart without repairs.

As this case of damage is apparently due to manufacturing rather than to EAC, there is no direct relevance to the topic under consideration here. However, it should also be noted that no surface cracks were detected during extensive examination after an operating period of more than 20 years, despite the direct and extensive surface contact between the LAS and steam condensate.

This once again provides evidence of the inherent SCC resistance of the LAS head material.

3.3.7 Damage to another BWR Pressure Vessel (Steam Converter)

Garigliano, Italy; GE BWR, 150 MWe, operating period 1963-1982.

In some BWR plants of early design, the reactor coolant system was separated by a heat exchanger from the actual steam, condensate and feedwater cycle in the turbine. This steam converter consisted of a vertical, cylindrical pressure vessel with spherical vessel heads. A lower tubesheet (sometimes, in straight tube variants, also an upper tubesheet) was welded into the vessel with several thousand heat exchanger tubes rolled and welded into place at the ends. Serious damage occurred in the steam converter in a plant of this type [3-7], as described in more detail below.

3.3.7.1 Type and Extent of Damage

After approximately 15 years of operation, a leak occurred in circumferential shell weld "J" in the lower area of the second steam converter (see Figure 3-12). The A302-B LAS of the pressure-retaining wall (thickness = 65 mm [2.6 inches]) was covered on the inside with an approximately 6 mm (0.24 inches) thick cladding of Monel 140 (Ni-Cu alloy, with an S content of 0.009%). NDE indicated extensive axial and radial cracking in this weld, extending an average of 30 to 50% through the wall. Further cracks were found in the adjacent circumferential weld "I" (Figure 3-12), as well as in weld "J" of the other steam converter. These other cracks were, however, restricted to the Monel cladding.

The cladding cracks were intergranular or interdendritic, while those in the LAS (base material and weld metal) were transgranular.

3.3.7.2 Cause and Mechanism of Damage

In addition to hot cracking, crack initiation was attributed to SCC in the Monel. Unusual manufacturing steps (complex sequence of automatic and manual welding with local stress-relief

heat treatment at approximately 620°C [1150 F]), which had led to considerable residual stresses, are regarded as having been significant.

Crack propagation in the low-alloy steel was also attributed to SCC [3-7]. In addition to the high stresses, the following points are considered significant here:

- High S content (up to 0.030%) in the LAS.
- High dissolved oxygen content (up to approximately 20 ppm) in the primary-side operating environment as a result of complete, forced condensation of live steam in the steam converter.

3.3.7.3 Derivable Crack Propagation Rate

The crack propagation rates in the steam converter base material were analyzed by Ford and Andresen [3-8] using the low-sulphur line of their film rupture/slip oxidation model. Only axial cracks were considered, as the stresses acting here could be better characterized. Based on the practical observation in the steam converter that crack depth had increased more rapidly than crack length, stress intensity factors were calculated with a mixed formula for $a/2c = 0.15$ to 0.30.

Two theoretical crack propagation curves were calculated (Figure 3-13) that bound the observed crack depths in weld J. The upper curve is based on the assumption of a pre-existing existing hot crack extending through the cladding on initial plant startup and an operating time corresponding to a 75% availability over approximately 90,000 h. In contrast, the lower curve assumes an initial crack depth of only 2.54 mm (0.1 in) in the cladding, so that nearly 60,000 hours of operation would have transpired before the low-alloy steel base material came into contact with the steam condensate.

The theoretical model on which this analysis is based yields conservative crack propagation rates of approximately 2×10^{-8} to 3×10^{-7} mm/s (2.8×10^{-6} to 4.2×10^{-5} in/h) for SCC in the low-alloy steel over the range of calculated K_I values of roughly 30 to 60 MPa $\sqrt{\text{m}}$ (27.3 to 54.5 ksi $\sqrt{\text{in}}$).

3.3.7.4 Remedial Action

The Garigliano plant was operated further until decommissioning in 1982 without a steam converter, i. e., the main steam was routed directly to the turbine, as is more usual in modern BWRs.

3.3.7.5 Relevance for Assessment of SCC in other BWR Plants

This case is not directly relevant to the evaluation of existing BWR plants for various reasons including the following:

- Non comparability of the materials used (especially with regard to the Monel cladding).
- Different manufacturing process for the steam converter vessel than for a RPV.
- Significant environmental difference between water with a very high oxygen content from complete steam condensation (dissolved oxygen content up to approximately 20 ppm) in the steam converter and reactor water or steam condensate with max. 0.3 ppm oxygen in the RPV of conventional BWRs.

3.4 Overall Assessment and Conclusion

Table 3-2 provides a summary of all cases of damage observed in the RPVs of BWR plants that might be considered relevant with regard to the SCC resistance of the materials of construction. Overall, the following conclusions can be drawn from the analysis of current knowledge regarding these cases:

3.4.1 *Austenitic Stainless Steel Cladding*

Manufacturing deficiencies, such as insufficient delta ferrite content, martensite formation or extensive cold-work due to incorrect grinding, can lead to IGSCC susceptibility in austenitic stainless steels exposed to reactor water or steam condensate. Cracks extending through the cladding have resulted over long operating periods in a limited number of cases.

However, even in cladding sensitized by heat treatment, SCC damage has been observed only for combinations of several unusual circumstances. In comparison with the wrought alloy, an unstabilized stainless steel cladding containing sufficient delta ferrite already offers higher SCC resistance under typical BWR conditions.

3.4.2 *Low-alloy Steel Base Material*

There are no cases of RPV damage in BWR plants that indicate susceptibility of the LAS base material to SCC during normal reactor operation. In contrast, certain cases indicate excellent SCC resistance under these conditions, since no corrosion damage in the form of cracks has occurred either as a result of extensive surface contact with the operating environment, (e. g. for unclad reactor heads or nozzle bore radii), or at the tips of cracks extending through the cladding. The pitting corrosion occasionally observed at the phase boundary between the stainless steel cladding and the LAS is insignificant and, in the fracture-mechanics sense, can even serve to blunt a crack growing through the cladding.

EAC (SICC: strain-induced corrosion cracking and corrosion fatigue) has been observed at the unclad feedwater nozzle of a German BWR as a result of fabrication deficiencies (weld root defects) and thermal loading (in particular, thermal stratification during hot standby). The absence of crack growth during normal, steady-state operation is further evidence for the resistance of LAS to SCC in good BWR water chemistry.

**Content Deleted -
EPRI Proprietary Information**

3.5 References

- 3-1. A. J. Giannuzzi, "Evaluation of Reactor Pressure Vessel Head Cracking in Two Domestic BWRs," EPRI, Final Report, TR-101971, Research Project C102-12, February 1993.
- 3-2. M. R. Fleming, A. P. L. Turner, J. A. Gorman, and R. W. Staehle "Review of Steam Generator Girth Weld Cracking," EPRI, Final Report, TR-103498, Research Project S407-52, December 1993.
- 3-3. E. A. Wimunc, "How Serious are Vessel Cladding Failures", Power Reactor Technology 9 (1966) 101 – 109.
- 3-4. S. H. Bush and R. L. Dillon "Stress Corrosion in Nuclear Systems," NACE Conference "Stress Corrosion and Hydrogen Embrittlement of Iron-Base Alloys," Firminy (1973), pp. 61 – 79.
- 3-5. T. Kondo, H. Nakajima and R. Nagasaki, "Metallographic Investigation on the Cladding Failure in the Pressure Vessel of a BWR," Nuclear Engineering & Design 16 (1971) 205 – 222.
- 3-6. C. W. Dillman, et al., "Boiling Water Reactor Feedwater Nozzle/Sparger Final Report," in: GE NEDO-21821, 78NED264, Class I, June 1978.
- 3-7. B. M. Gordon, D. E. Delwiche and G. M. Gordon, "Service Experience of BWR Pressure Vessels," "Performance of Light-Water Reactor Pressure Vessels," ASME PVP Vol. 119, Ed. R. Rungta, J. D. Gilman and W. H. Bamford, San Diego, June 1987.
- 3-8. F. P. Ford and P. L. Andresen, "Stress Corrosion Cracking Of Low-Alloy Pressure Vessel Steels In 288°C Water," 3. I.A.E.A. Specialists "Meeting on Subcritical Crack Growth," Moscow, 14.-18.5.90; Published as NUREG Report CP-0112, ANL-90/22 (August 1990), Vol. 2, pp. 37-57.
- 3-9. P.C. Riccardella, J. F. Copeland and J. Gilman, "Evaluation of Flaws or Service Induced Cracks in Pressure Vessels," "Performance of Light-Water Reactor Pressure Vessels," ASME PVP Vol. 119, Ed. R. Rungta, J. D. Gilman and W. H. Bamford, San Diego, June 1987.
- 3-10. R. E. Smith, R. Hanford and S. C. Cheng, "Pressure Vessel Nozzle Repair," Nuclear Engineering and Design 124 (1990) 79-90.
- 3-11. S. C. Cheng, "Overview of Chinshan Nuclear Power Station Recirculation Pipe Repair and Replacement," NUREG / CP – 0109 (1990), pp. 299–336.

- 3-12. EPRI Report No. TR-108710, BWR Vessel and Internals Project, "Evaluation of Crack Growth in BWR Nickel Base Austenitic Alloys in RPV Internals (BWRVIP-59)," EPRI Proprietary, December 1998.
- 3-13. K. Kussmaul et al., "Formation and Growth of Cracking in Feed Water Pipes and RPV Nozzles," Nuclear Engineering and Design 81 (1984) 105-119.
- 3-14. E. Lenz and N. Wieling, "Strain-Induced Corrosion Cracking of Low-Alloy Steels in LWR-Alloy Steels in LWR-Systems – Interpretation of Susceptibility by Means of a Three Dimensional (T, $d\epsilon/dt$, Dissolved Oxygen) Diagram," Nuclear Engineering and Design 91 (1986) 331-344.
- 3-15. J. Hickling, "Strain-Induced Corrosion Cracking: Relationship to Stress Corrosion Cracking / Corrosion Fatigue and Importance for Nuclear Plant Service Life," Proc. 3rd IAEA Specialists' Meeting on Sub-Critical Crack Growth, Moscow, May 1990; Pub. NUREG/CP-0112, ANL-90/22, Vol. II, pp. 9-26 (1990).

Table 3-1

Ultrasonic indications at Brunswick Unit 1 recirc inlet safe-end-to-nozzle welds [3-10]

Pre-overlay				Post-overlay			
Nozzle	Finding	Maximum % thru-wall	Maximum length (in.)	Nozzle	Finding	Maximum % thru-wall	Maximum length (in.)
A	2 Axials	50	0.40	A	1 Axial	60	0.40
B	2 Axials	45	0.45	B	2 Axials	45	0.40
C	4 Axials	37	0.30	C	1 Axial	50	0.25
D	6 Axials	82	0.55	D	6 Axials	100	1.70
E	10 Axials	65	0.55	E	7 Axials	81	0.85
G	4 Axials	52	0.25	G	2 Axials	95	0.30
H	11 Axials	71	0.60	H	10 Axials	100	1.50

Table 3-2
Overview of RPV degradation in BWR-Plants

**Content Deleted -
EPRI Proprietary Information**

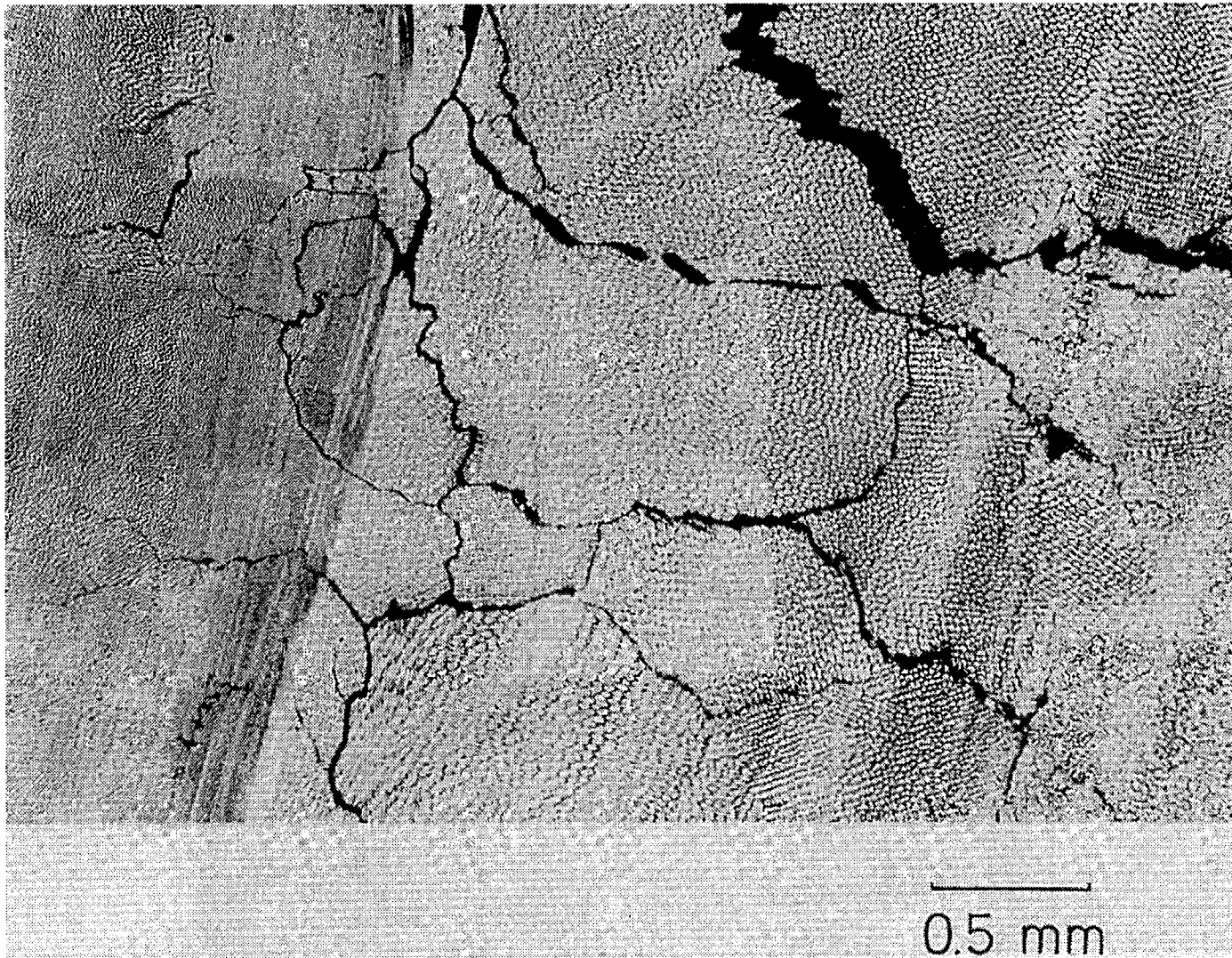


Figure 3-1. Intergranular Cracks in the Austenitic Cladding of the JPDR - Optical Micrograph of a Sectional Plane [3-5]

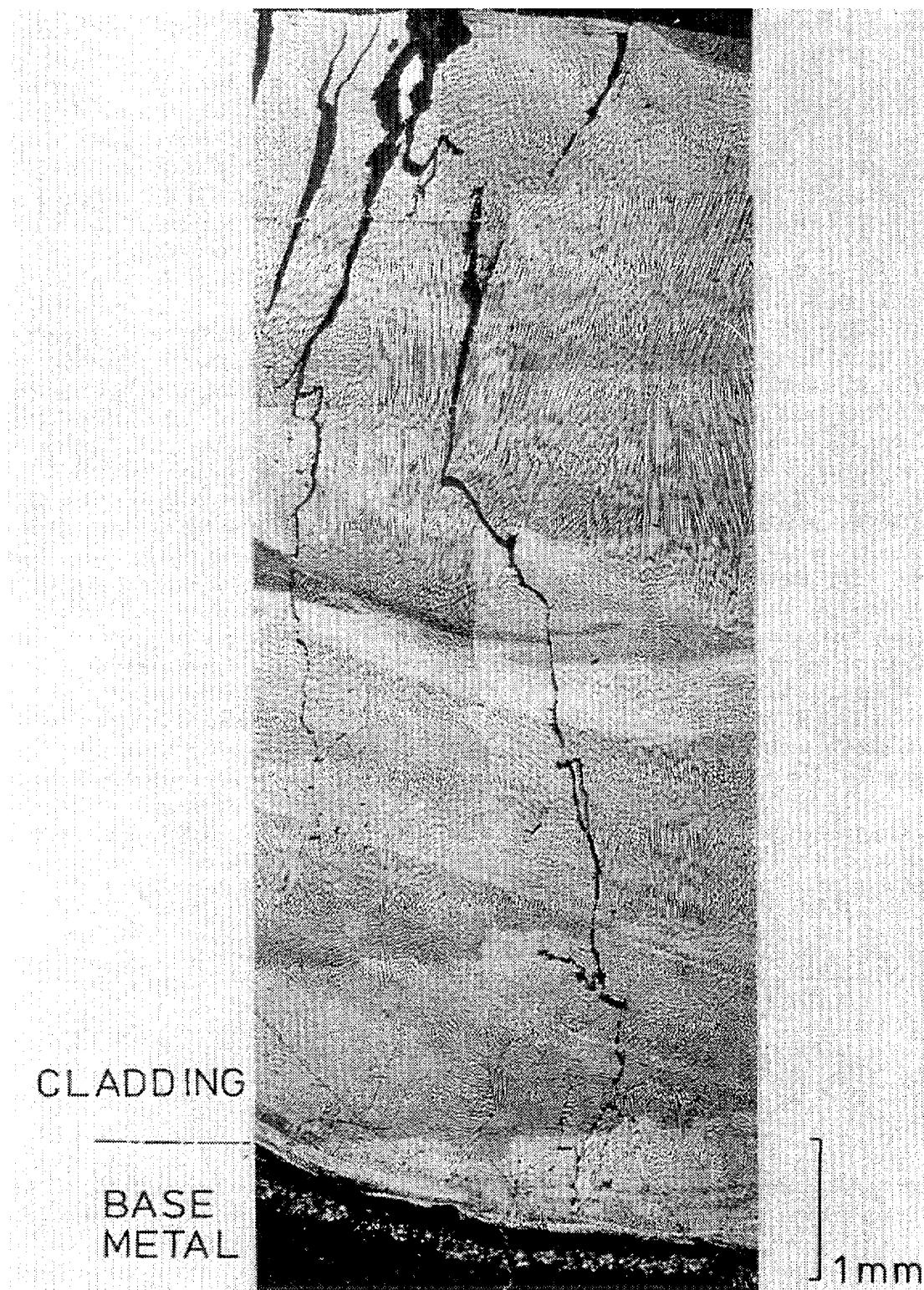


Figure 3-2. Transgranular Cracks in the Austenitic Cladding of the JPDR – Optical Micrograph of a Sectional Plane [3-5]



Figure 3-3. Pitting Corrosion at the Crack Tip in the Austenitic Cladding of the JPDR [3-5]

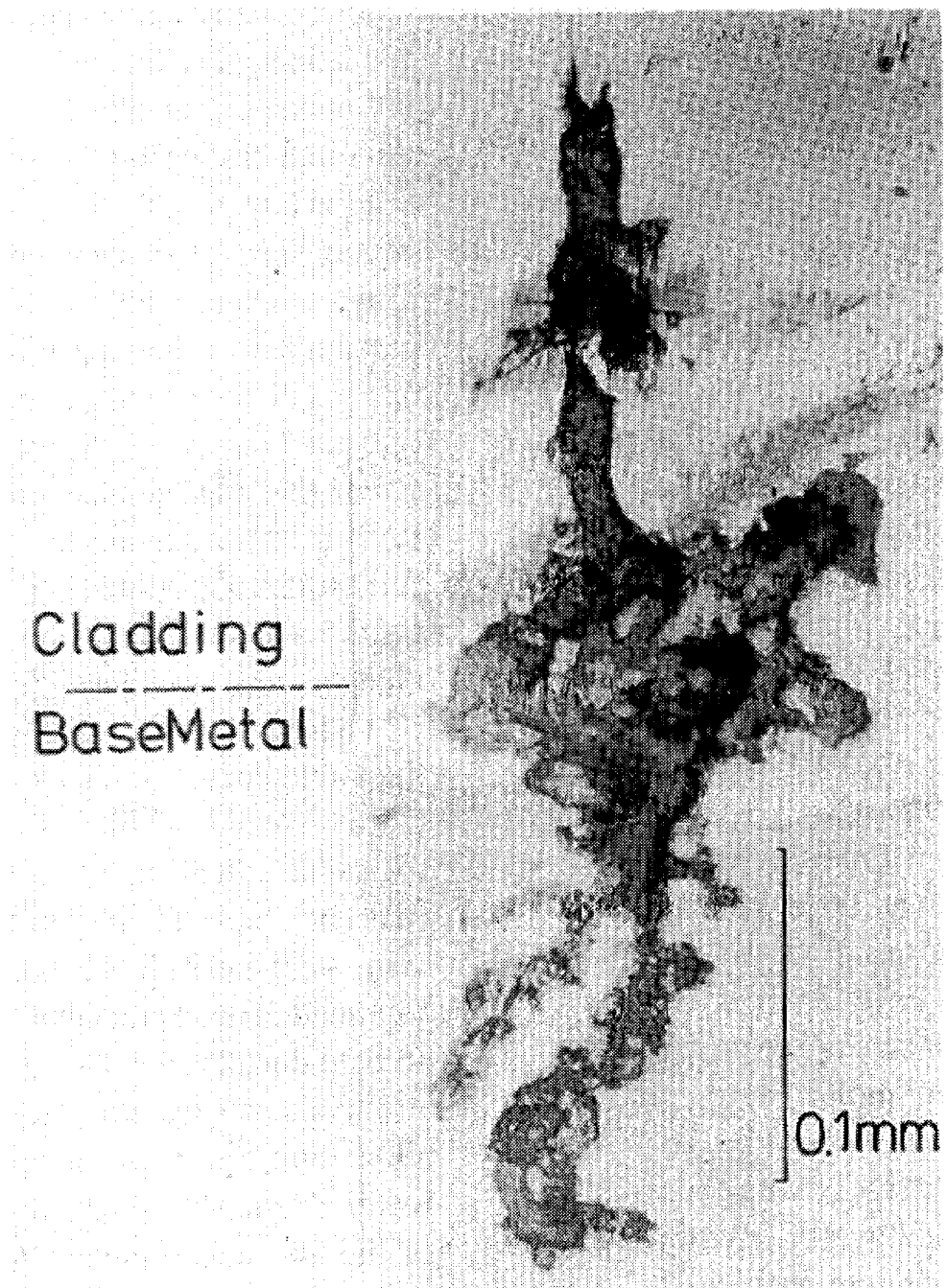


Figure 3-4. Pitting Corrosion at the Crack tip in the Austenitic Cladding of the JPDR [3-5]

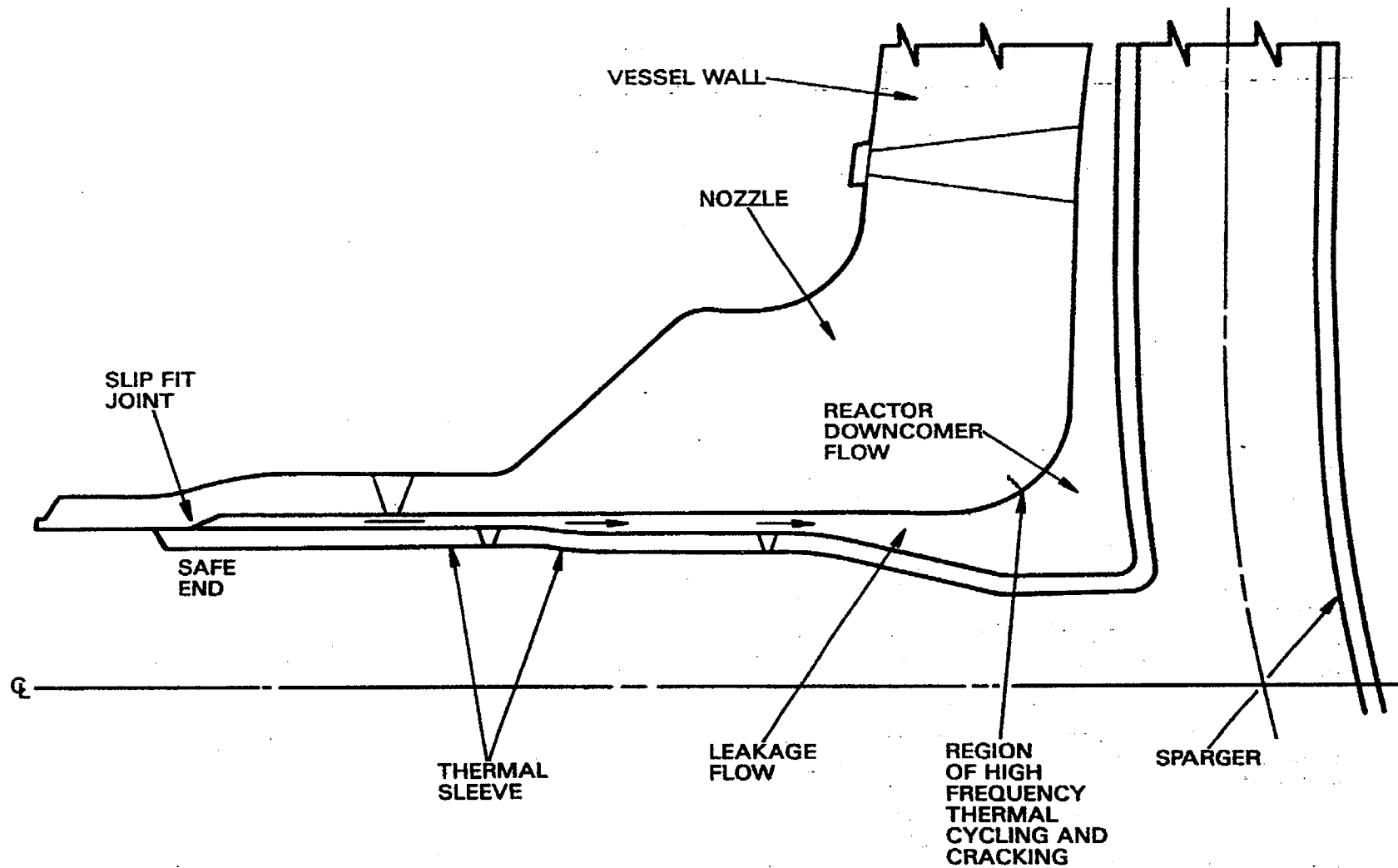


Figure 3-5. Location of Cracks in Feedwater Nozzle - Cross Section [3-7]

**Content Deleted -
EPRI Proprietary Information**

Figure 3-6. Comparison of Observed and Calculated Crack Lengths [3-6]

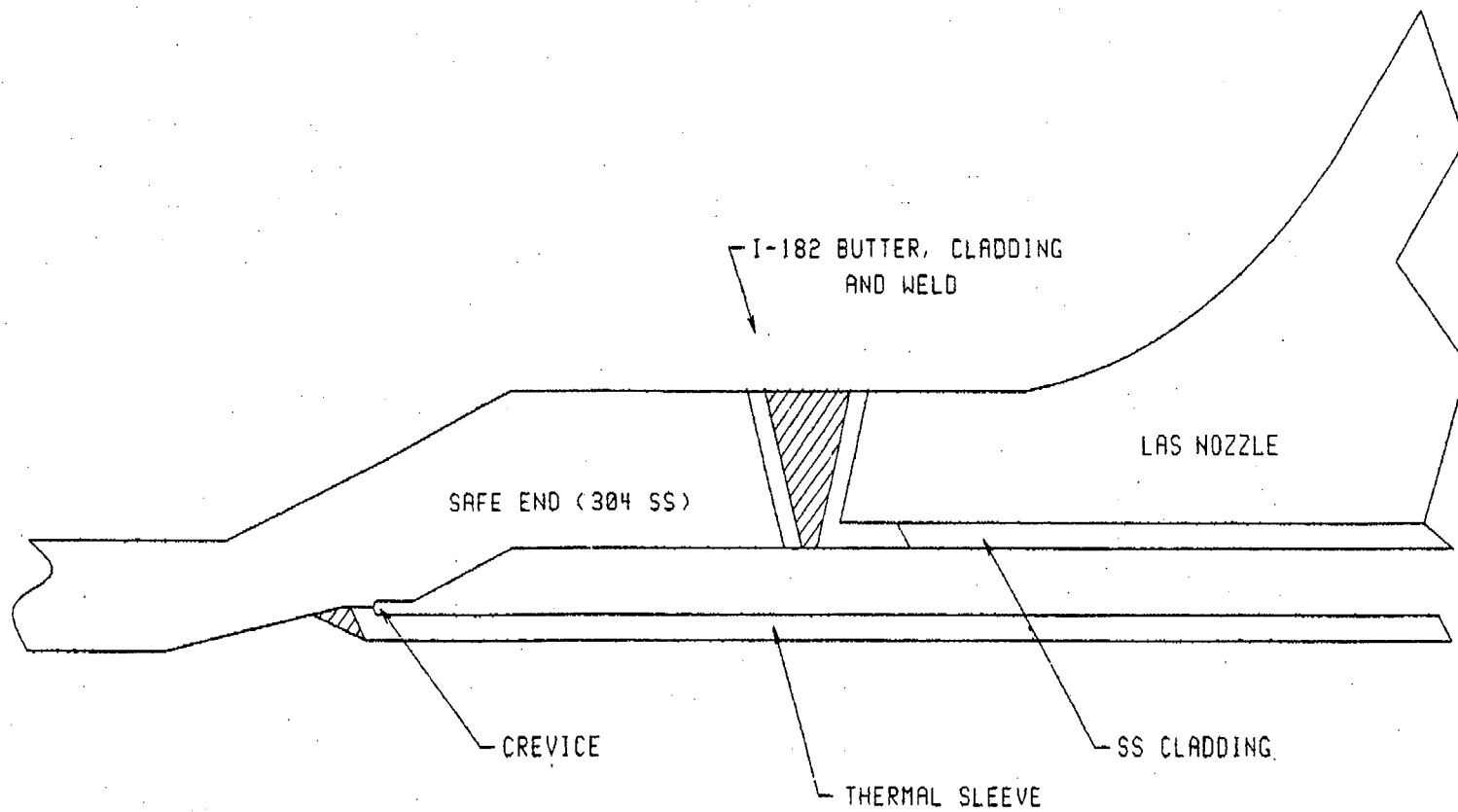


Figure 3-7. Old Safe End/Nozzle Configuration [3-10]

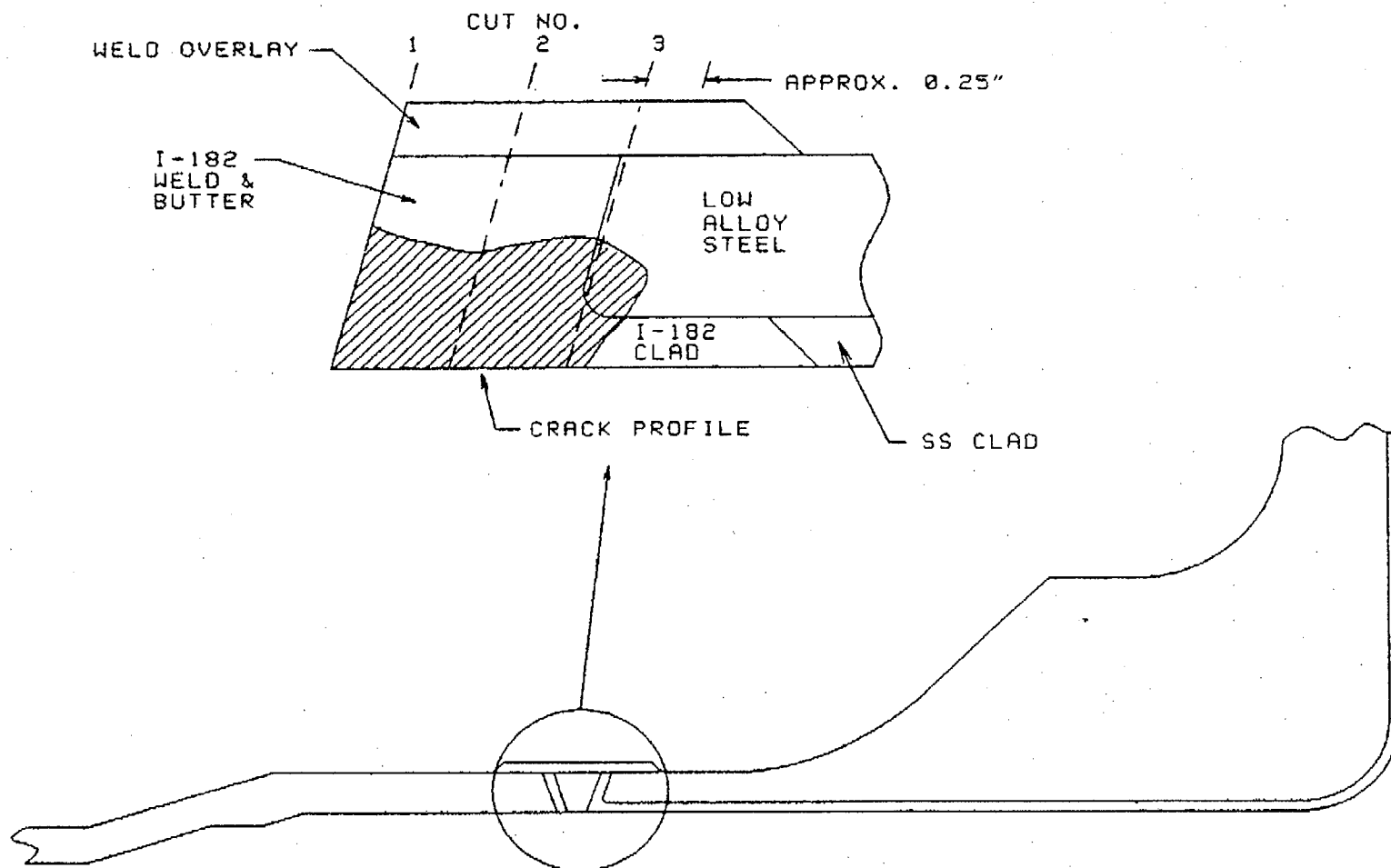


Figure 3-8 Crack Profile - Chinshan 2 N2E Nozzle (Recirculation Inlet) [3-10]

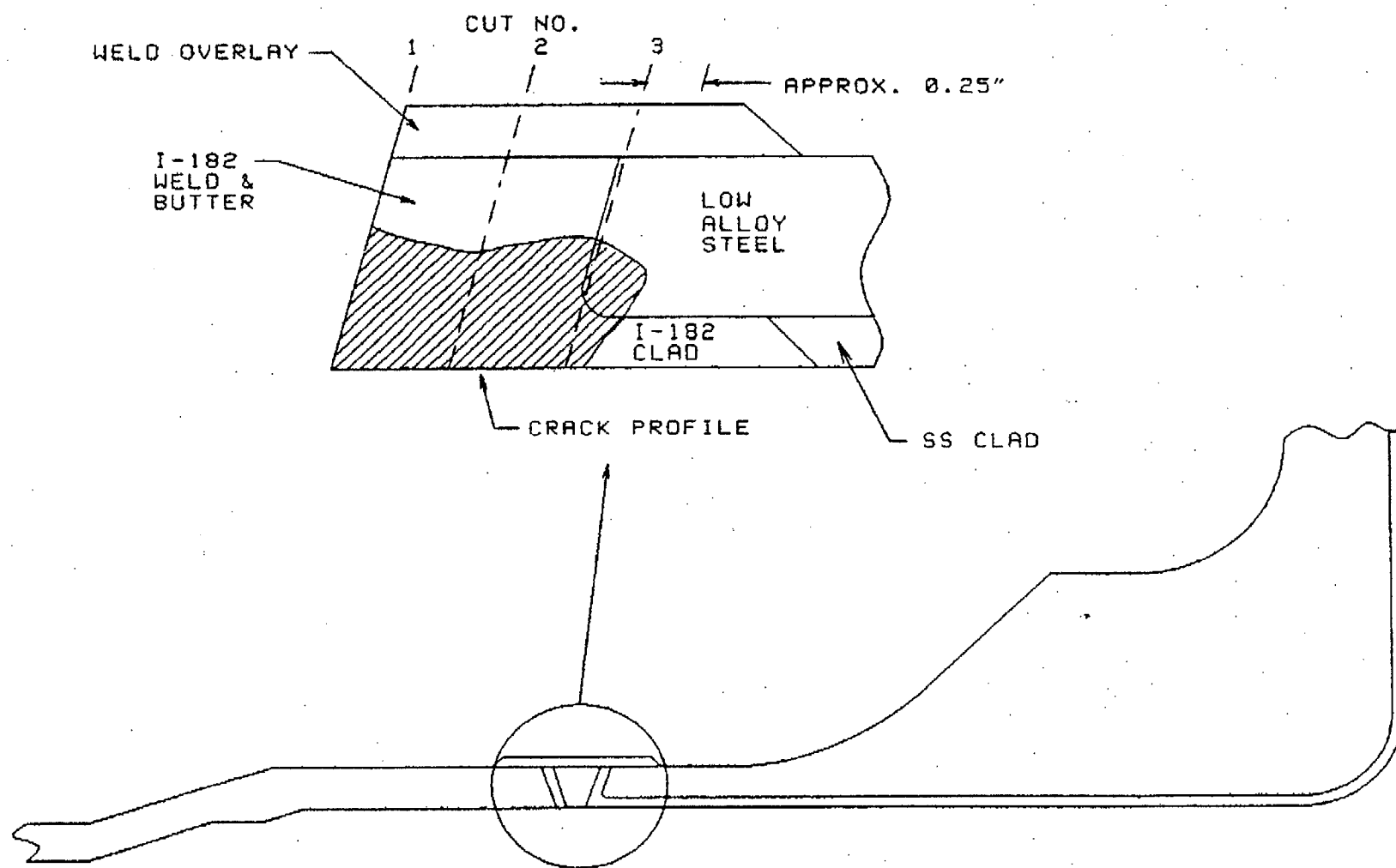


Figure 3-9. Typical Location of Ultrasonic Inspection Indications in Nozzle/Safe-end Weldment at Brunswick Unit 1 before Weld Repair [3-10]

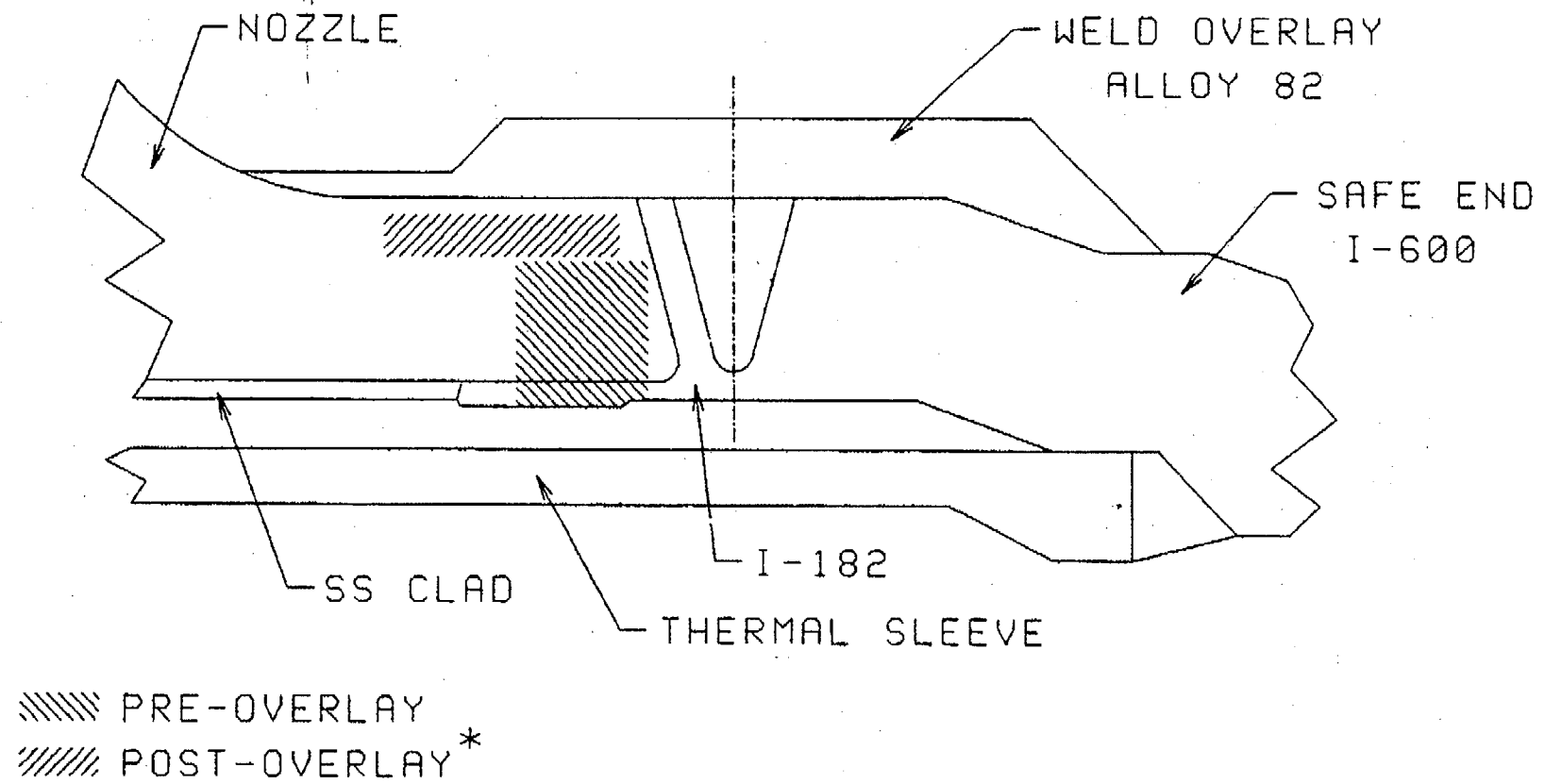


Figure 3-10. Typical Location of Ultrasonic Inspection Indications in Nozzle/Safe-end Weldment at Brunswick Unit 1 after Weld Repair [3-10]

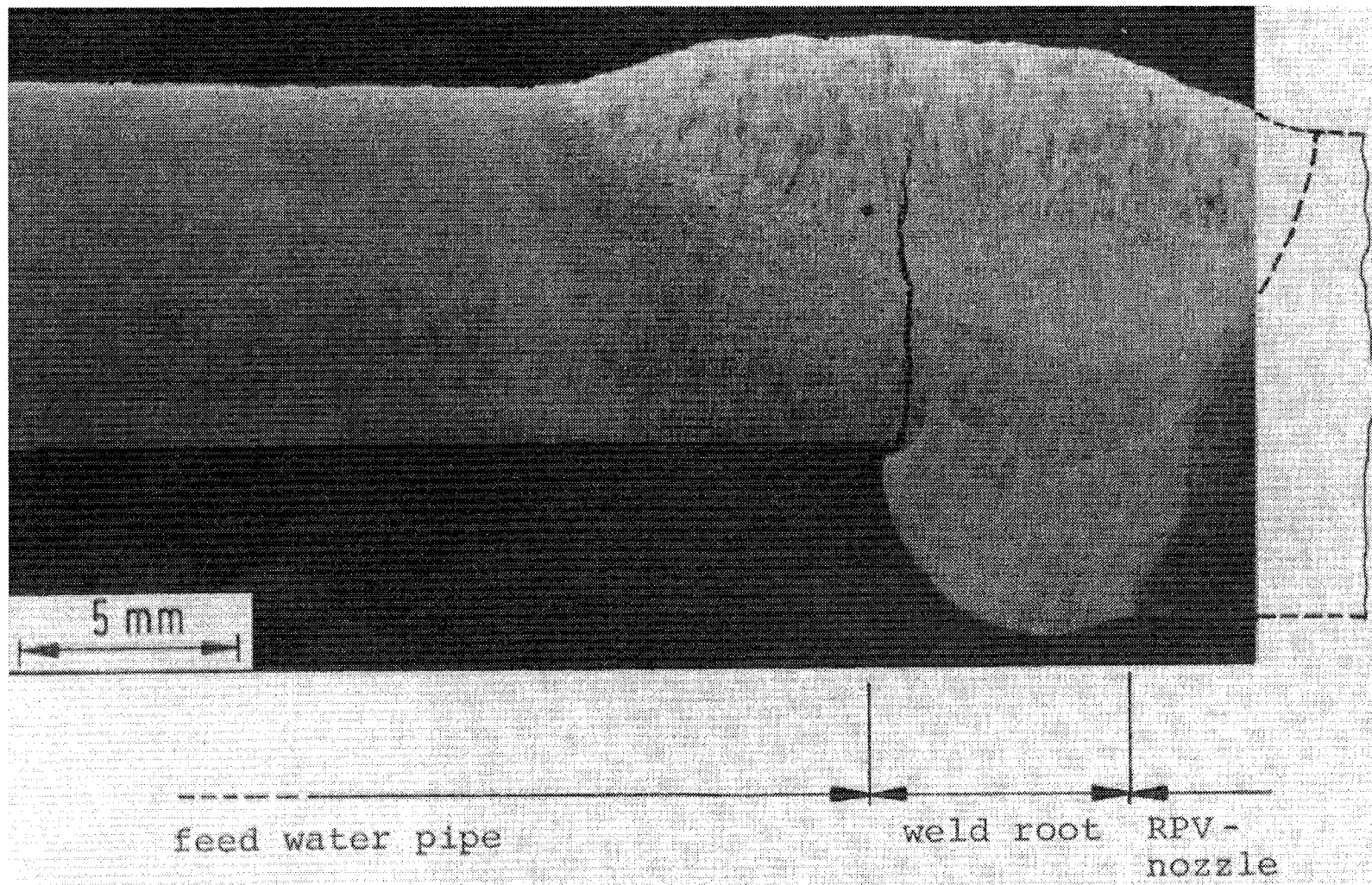


Figure 3-11. Cracking in the Feedwater Piping of a BWR Adjacent to the RPV Nozzle [3-13]

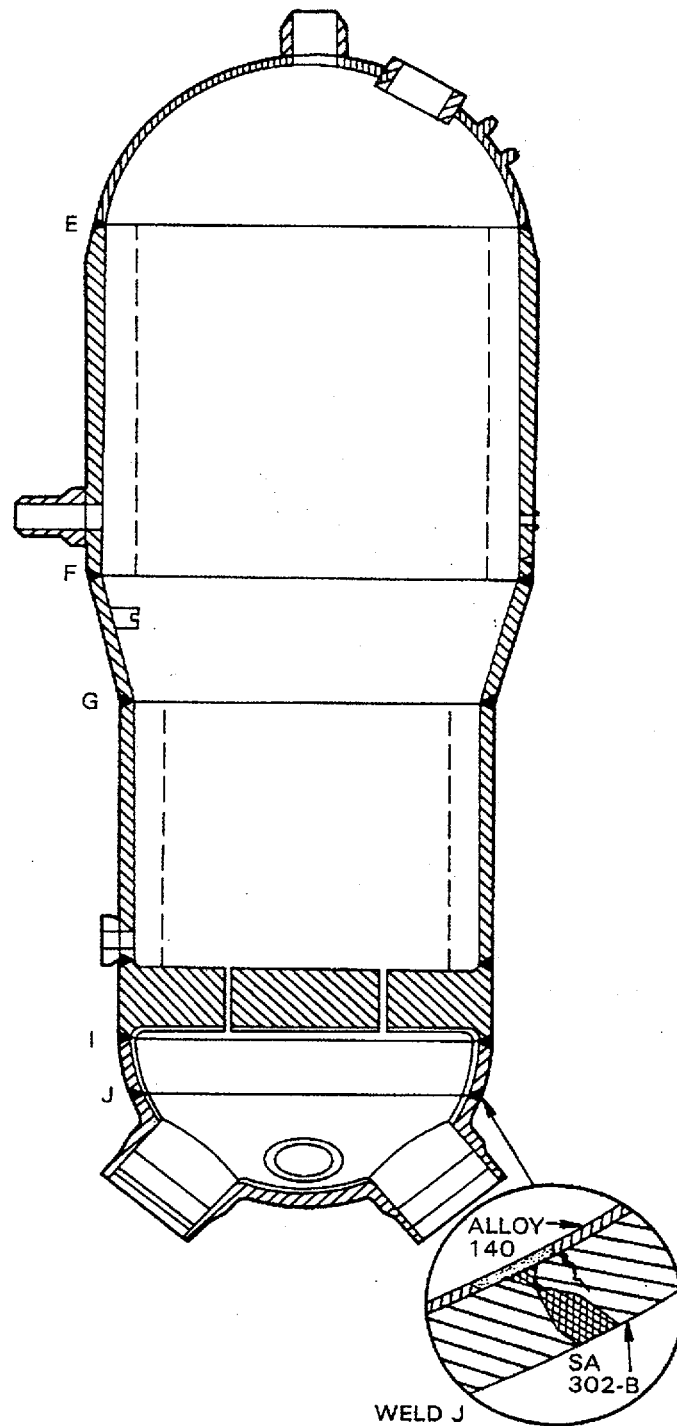


Figure 3-12. Location of Cracks in Weld J of the Garigliano Steam Converter – Cross Section
[3-7]

PREDICTIONS AND OBSERVATION FOR SA302
CRACKING AT GARIGLIANO SG
AXIAL CRACKS AT WELD J

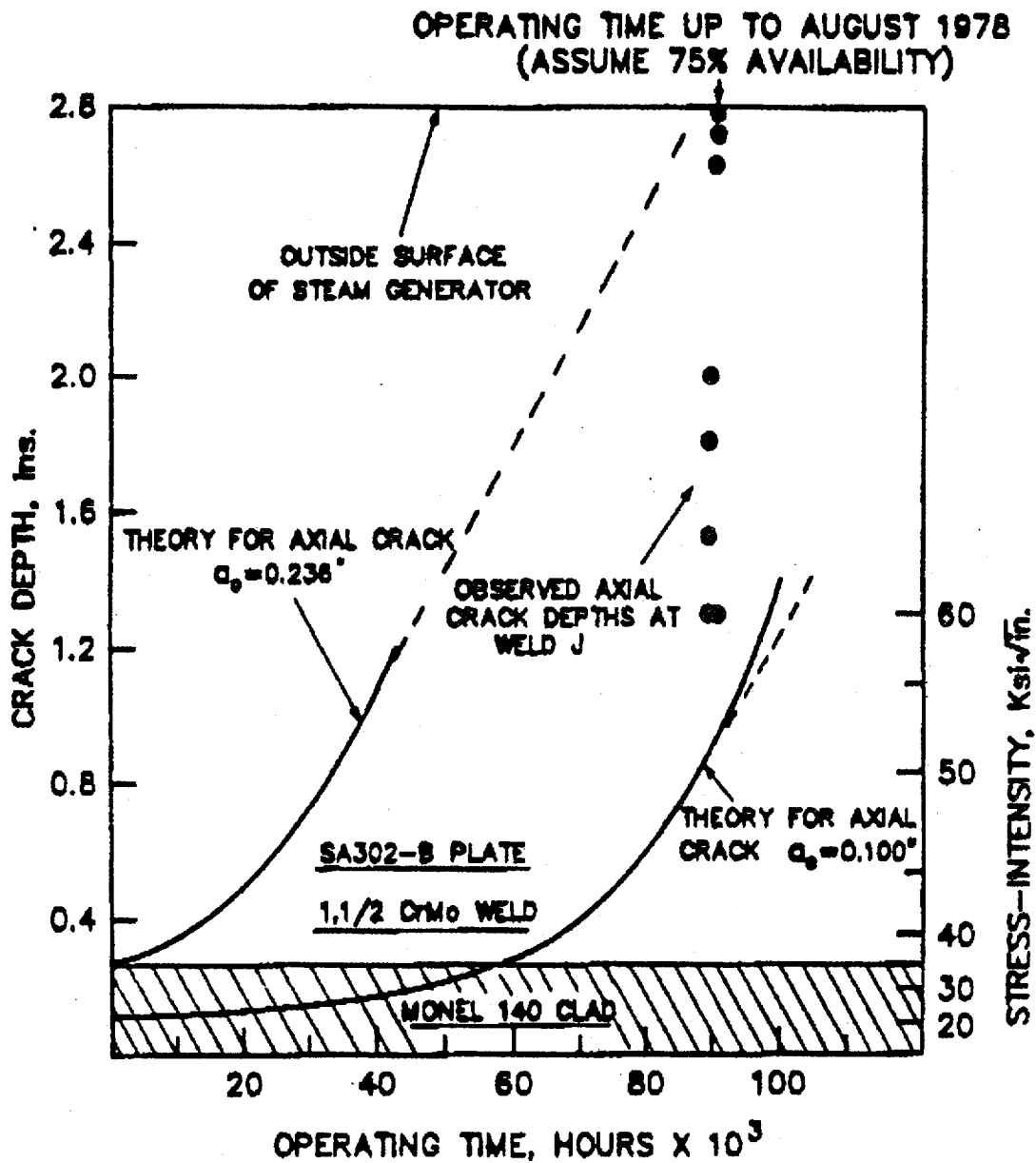


Figure 3-13. Theoretical Crack Depth/Operating Time Relationships for the Garigliano Steam Converter [3-8]

4.0 STRESS CORROSION CRACKING OF LOW ALLOY STEEL IN BWR WATER: LABORATORY STUDIES

The purpose of this section is to review the current state of understanding of SCC in LAS based on data from laboratory size test specimens. Much of the data has been available for many years. GE performed much of the testing in the late 1970s and early 1980s although other investigators also performed studies in that time period. This data is reviewed in section 4.1. In 1992, EPRI sponsored a study at GE in conjunction with other laboratories to perform additional well-controlled testing to better understand the cyclic loading and water transient conditions necessary to produce cracking in these alloy steels. This was deemed necessary based on excellent field experience that has continued to confirm that LAS are highly resistant to SCC under constant load conditions and exposed to NWC BWR environments. This effort included laboratory testing as well as confirmatory reactor site testing. This work is summarized in 4.2. The reactor site data, unreported to date, is discussed more extensively in section 4.3. Section 4.4 provides a brief discussion of important new data from Materialprüfungsanstalt (MPA) Stuttgart and from the Paul Scherrer Institute. Section 4.5 then summarizes all the data in the context of its relevance to crack growth modeling and disposition curves.

4.1 Old Laboratory Results from GENE

The majority of the early constant load tests of LAS testing conducted in autoclaves under BWR type oxygenated water at 288°C (550°F) with some flow were conducted by GE Nuclear Energy and GE CR&D. These tests employed bolt-loaded wedge-open-load (WOL)-type specimens that were displacement controlled tests as well as compact-tension (CT)-type or double cantilever beam (DCB) type specimens that were conducted under load control. The results of these different tests, summarized in Reference 4-1, will be briefly discussed below.

Several investigators used displacement controlled tests to evaluate the general susceptibility of the LASs to SCC. These early tests were conducted in both 0.2 ppm to 8 ppm oxygenated environments with high conductivity, generally 0.5 to 1.0 $\mu\text{S}/\text{cm}$ levels. The specimens were

loaded over a range of K levels as well (up 121 MPa $\sqrt{\text{in}}$ [110 ksi $\sqrt{\text{in}}$]). Growth was observed, particularly at high K values. Interpretation was complicated due to the load relaxation that occurred during the testing period.

**Content Deleted -
EPRI Proprietary Information**

4.2 Previous Results from GENE GE CR&D: EPRI RP C102-4

A collaborative research effort was undertaken to further assess the SCC characteristics of LAS in BWR primary reactor water environments. The major efforts were directed toward experimental measurements of SCC crack propagation rates. This work was performed by several different laboratories, with GENE the lead organization for the program. The main laboratories in addition to GENE included GE CR&D, Hitachi, Toshiba and Tohoku University. The program was initiated with a round robin test program to establish that the different laboratories would be capable of developing comparable data. This effort set specific mechanical and environmental parameters that had to be followed to demonstrate this inter-laboratory consistency. This work was completed in 1994 and was reported in Reference 4-3.

**Content Deleted -
EPRI Proprietary Information**

**Content Deleted -
EPRI Proprietary Information**

**Content Deleted -
EPRI Proprietary Information**

4.3 Recent Reactor Site Testing Data

This test program was the final phase of RP C102-4 and represents new data. The program is fully detailed in Appendix A.

**Content Deleted -
EPRI Proprietary Information**

**Content Deleted -
EPRI Proprietary Information**

**Content Deleted -
EPRI Proprietary Information**

4.4 Other Testing Results

There are two other, major, research programs that also contribute to understanding the susceptibility of low alloy steel to SCC crack growth in BWR environments. Work reported by Kussmaul, Blind and Laepple of the MPA-Stuttgart (Reference 4-4) assessed the crack growth rates observed over periods of up to approximately 1000 h in German low alloy steel similar to A508 class 2 and A533B materials during exposure to oxygenated water, primarily at a somewhat lower temperature (240°C [464°F]). Unfortunately, their attempts to monitor crack

growth on-line via COD measurements were only effective at high K_1 levels.

**Content Deleted -
EPRI Proprietary Information**

**Content Deleted -
EPRI Proprietary Information**

The other major research program on SCC of LAS, not yet completed, is the work being performed by Seifert and colleagues at the Paul Scherrer Institute (PSI) in Switzerland (Reference 4-5).

**Content Deleted -
EPRI Proprietary Information**

4.5 Summary of Test Results

As indicated in the previous sections there have been investigations for more than 20 years into defining the SCC growth rate vs stress intensity relationships for LAS pressure vessel alloys in environments relevant to BWRs. The resultant crack growth rates have exhibited an extremely wide range, due to the large number of interacting system variables that can affect the cracking behavior, and which were not always adequately controlled during the testing. These factors have included:

**Content Deleted -
EPRI Proprietary Information**

Thus the following conclusions on the data trends are based on engineering judgment, backed up by these criteria as well as considerable amount of quantitative understanding of the mechanism of cracking in these low alloy steel/high temperature water systems (addressed in Section 5).

**Content Deleted -
EPRI Proprietary Information**

**Content Deleted -
EPRI Proprietary Information**

**Content Deleted -
EPRI Proprietary Information**

4.6 References

- 4-1. "Summary Overview of GE Low Alloy Steel SCC Data," K. S. Brown, PMWG-590, dated 9/20/91.
- 4-2. F. P. Ford, "Environmentally Assisted Cracking in Low Alloy Steels," EPRI NP-7473L, January 1992.
- 4-3. "Stress Corrosion Cracking in Low Alloy Steels, Interim Technical Report," prepared for EPRI by GE Nuclear Energy on EPRI Contract No. RP C102-4, dated February 1994.
- 4-4. "New Observations on the Crack Growth of Low Alloy Nuclear Grade Ferritic Steels under Constant Active Load in Oxygenated High-Temperature Water," K. Kussmaul, D. Blind and V. Laepple; Nuclear Eng. and Design, 168, pp. 53-75, 1997.
- 4-5. H. P. Seifert, J. Heldt and U. Ineichen: private communication to Dr. R. Pathania/EPRI.
- 4-6. J. Hickling: "Evaluation of Acceptance Criteria for Data on Environmentally Assisted Cracking in Light Water Reactors," SKI Report 94:14, dated September 1994.
- 4-7. A. Van der Sluys and R. Emmanuelson, "Enhancement of Fatigue Crack Growth Rates in Pressure Vessel Boundary Materials Due to Light Water Environments," Nucl. Eng. & Des. 119, 379-388, 1990.

Table 4-1 Test Results: RP C1024 Appendix III: GE Nuclear Energy Six Specimen Test

**Content Deleted -
EPRI Proprietary Information**

Table 4-2 Summary of Different Test Time Periods (CAV Test)

**Content Deleted -
EPRI Proprietary Information**

Table 4-3 Crack Growth Results (Crack Growth Rates in inch/hour)

**Content Deleted -
EPRI Proprietary Information**

**Content Deleted -
EPRI Proprietary Information**

Figure 4-1: Crack propagation rate vs. stress intensity relationships in flowing water containing 200 ppb dissolved oxygen at 288°C (550°F) for constant load type specimens (Reference 4-1, 4-2): all levels of conductivity (including $>0.5 \mu\text{S}/\text{cm}$). (Note: Reference designations are from Reference 4-2).

**Content Deleted -
EPRI Proprietary Information**

Figure 4-2: Crack propagation rate vs. stress intensity relationships in flowing 288°C (550°F) water with 200 ppb dissolved oxygen for constant load type tests
(Reference 4-1, 4-2): water conductivity restricted to $<0.5 \mu\text{S}/\text{cm}$. (Note: reference designations are from Reference 4-2).

**Content Deleted -
EPRI Proprietary Information**

Figure 4-3. Summary of Results of Round Robin Test: RPC102-4

**Content Deleted -
EPRI Proprietary Information**

Figure 4-4: Crack Growth of Low Alloy Steel: Four Phases of Loading in GENE Eight Specimen Test ($1 \text{ cm/s} = 1.4 \times 10^3 \text{ in/h}$)

**Content Deleted -
EPRI Proprietary Information**

Figure 4-5: Summary of Results of Latter Phases of Eight Specimen Test for Trapezoidal Loading: RP C102-4

**Content Deleted -
EPRI Proprietary Information**

Figure 4-6: Crack length and conductivity as a function of time for reversing DC Specimen LAS 89

**Content Deleted -
EPRI Proprietary Information**

Figure 4-7: CAV crack growth rates plotted for each material and test period. The rates in periods 5, 6 and 7 are very low, nearing the resolution limit.

**Content Deleted -
EPRI Proprietary Information**

Figure 4-8: Apparent crack growth rates determined by MPA-Stuttgart together with their chosen bounding line and the GE theoretical lines. Note that the bounding line at the lower K values is set by 1000 hr test time data.

5.0 CURRENT CRACK PROPAGATION RATE/STRESS INTENSITY DISPOSITION RELATIONSHIPS AND THEIR DERIVATION

5.1 Working Hypothesis for the Stress Corrosion Cracking Mechanism in the Low-Alloy Steel/Water System at 288°C (550°F): Film Rupture/Slip-Oxidation Mechanism

Various crack advancement theories have been proposed relating crack propagation to oxidation at the crack tip and the stress/strain conditions in that region, and these theories have been supported by a correlation between the average oxidation current density on a straining surface and the crack propagation rate for a number of systems. There have been various hypotheses for the precise atom-atom rupture process at the crack tip; for example, the effect that the environment has on the ductile-fracture process. The experimentally validated elements of these earlier proposals have been incorporated into the current film ruptures/slip-oxidation model. This model relates the crack propagation to the oxidation that occurs when the protective film at the crack tip is ruptured. The increase in crack tip strain necessary for the film rupture event may be related to a monotonically increasing or cyclic stress, or to the creep process in the underlying metal matrix under constant stress. Thus, the model is conceptually applicable to "stress corrosion", "strain induced cracking" and "corrosion fatigue". Once the film is ruptured crack tip advance is governed by oxidation on the bared surface, dissolution of the exposed metal matrix and film reformation. Because film formation will generally occur, the oxidation rate and hence crack penetration will slow with time. Thus, continued crack advance will depend on a further oxide rupture process due to the action of a strain rate at the crack tip. Therefore, for a given crack tip environment, potential, and material condition, the crack propagation rate will be controlled by both the change in oxidation charge density with time and the frequency of film rupture at the strained crack tip. The details of the model dependencies and quantification of the different parameters have been presented in detail in earlier reports [5-1 and 5-2].

Thus, the crack propagation rate/crack tip strain rate relationship may be generalized by:

$$\bar{V}_t = A \dot{\epsilon}_{ct}^n \quad (1)$$

where \bar{V}_t is the average environmentally controlled crack propagation rate, $\dot{\epsilon}_{ct}$ is the crack tip strain rate, and A and n are constants depending on the material and environment compositions at the crack tip. There are limits to the validity of this relationship, however, which are observed at high and low crack tip strain rates. At low crack tip strain rates, the ultimate criterion is that sharp cracks cannot be maintained when the average crack tip propagation rate, \bar{V}_t , approaches the oxidation rate on the crack sides, V_s . Under these conditions, therefore, the crack propagation rate will slow down with exposure time and crack arrest will eventually occur due to blunting. Later in this review other limiting criteria at low crack tip strain rates are discussed which are specific to the low-alloy steel/water system. At high crack tip strain rates, ($\sim 10^{-2}/s$), a bare surface is continuously maintained at the crack tip, and the environmentally controlled crack propagation rates becomes independent of $\dot{\epsilon}_{ct}$, since it cannot exceed the Faradaic equivalent of the bare surface dissolution rate.

Under either constant or monotonically increasing load conditions, the stress corrosion crack propagation rate is defined by Equation 1. Under cycle loading conditions, however, the crack is moving forward by irreversible cyclic plastic deformation, e.g. fatigue striation formation. Since this mechanical crack advance is occurring independently of the crack advance by oxidation processes, these two crack advance mechanisms, (striation formation and oxidation) are considered additive.

5.2 Development of the High Sulfur and Low Sulfur Crack Growth Prediction Algorithms for Low-Alloy Steel/Water Systems at 288° C (550° F)

To derive the equations and constants from first principles, it is necessary to measure the oxidation rates for alloy/environment systems expected at the strained crack tip. The current knowledge of such fundamental determinations for low-alloy steel/water systems has been reviewed in References 5-1 through 5-4. The key developments are as follows.

**Content Deleted -
EPRI Proprietary Information**

**Content Deleted -
EPRI Proprietary Information**

5.3 Comparison of Observed and Predicted Stress Corrosion Crack Propagation Rates in LAS/Water Systems At 288 °C (550 °F)

The comparison between observed and predicted SCC propagation rates is usually conducted in three logical phases: (a) laboratory data on precracked fracture mechanics-type or slow strain rate specimens, (b) field experience where cracking of the LAS has occurred because of propagation of a pre-existing crack through an overlay cladding and (c) general experience of cracking of LASs in LWRs. Only a review of the laboratory data from section 4.0 will be discussed since the field data have established that LAS has excellent behavior in the high purity, operating environments.

Although thoroughly covered in Reference 4-2, it is important to first re-visit the crack propagation rate/stress intensity data for low alloy steels in 6-8 ppm oxygenated water at 288°C (550° F) under constant load and displacement. These data form the upper bound of the data due

to the test conditions.

**Content Deleted -
EPRI Proprietary Information**

**Content Deleted -
EPRI Proprietary Information**

5.4 Interim Recommendations on Disposition Relationships

Currently there are two potential crack propagation rate vs stress intensity disposition relationships that might be proposed for LASs in high temperature water, and which have some fundamental understanding to support their formulation:

**Content Deleted -
EPRI Proprietary Information**

5.4.1 *Basis for Disposition Line Positioning*

**Content Deleted -
EPRI Proprietary Information**

**Content Deleted -
EPRI Proprietary Information**

5.4.2 *Disposition Line: Constant Load*

**Content Deleted -
EPRI Proprietary Information**

5.4.3 *Disposition Line: Water Chemistry and Load Transients*

**Content Deleted -
EPRI Proprietary Information**

5.5 References

- 5-1. F. P. Ford, D.F. Taylor, P.L. Andresen and R. G. Ballinger, "Corrosion-Assisted Cracking of Stainless and Low Alloy Steels in LWR Environments," EPRI Contract RP 2006-6, Report NP5064M, February 1987.
- 5-2. F. P. Ford, "Environmentally Assisted Cracking in Low Alloy Steels," EPRI NP-7473L, January 1992.
- 5-3. F.P. Ford and P.L. Andresen, "Stress Corrosion Cracking of A533B/Pressure Vessel Steels in Water at 288 C," Proc. Third Intl. Atomic Energy Agency Specialists Mtg. On Subcritical Crack Growth, Moscow, USSR, May 1990, NRC NUREG/CP-0112 (ANL-90/22), Vol. 2, pp. 37-54.
- 5-4. F.P. Ford, D. Weinstein and S. Ranganath, "Stress Corrosion Cracking of Low Alloy Steels in High Temperature Water," Proc. Fifth Intl Sym. on Environmental Degradation of Materials in Nuclear Power Systems-Water Reactors, Monterey, ANS, 1992, pp. 561-570.

**Content Deleted -
EPRI Proprietary Information**

Figure 5-1. BWRVIP Disposition Lines: Line for (a) Constant load and (b) Transient and Loading conditions shown.

6.0 OPERATIONAL AND RESIDUAL STRESS DETERMINATION, AND FRACTURE MECHANICS CONSIDERATIONS

Stresses associated with BWR attachment welds can be classified into fabrication and operational stresses. Fabrication stresses consist of weld residual stresses resulting from welding the vessel plates, clad stresses due to the application of the clad and subsequent post weld heat treatment, and the stresses resulting from the attachment weld. Operational stresses are those associated with the normal operation of the plant and consist of stresses analyzed in the ASME Code stress reports. These include dead weight, pressure, thermal and seismic loads.

This section of this report describes the residual stress distributions for vessel cladding and for one important vessel attachment, the shroud support attachment, designated H9. Experimental and analytical weld and clad residual stresses are presented for these locations. Based upon the residual stresses developed, through-wall stress intensities are presented for the various residual stress distributions.

6.1 Vessel Clad Residual Stresses

Cladding of the vessel results in tensile residual stresses in the clad material and compressive stress in the vessel plate material beneath the clad. To reduce the residual stresses in the clad vessel, a post weld heat treatment stress relief process is applied following application of the cladding. This is achieved by subjecting the entire clad vessel to a temperature of approximately 540 to 650°C (1100° to 1200°F) for 12 to 48 hours and then gradually cooling it uniformly to room temperature. At the stress relieving temperature of 540 to 650°C (1100-1200°F), it is expected that the vessel and cladding will be essentially stress-free. However, during cooling to room temperature tensile residual stresses are generated in the stainless steel cladding because stainless steel has a higher coefficient of thermal expansion than the low alloy pressure vessel material.

The magnitude and distribution of the clad stress before and after stress relief have been investigated by many researchers. An excellent summary of all the work done by various

researchers [6-1 to 6-7] has been presented by Rybicki et al., [6-8]. All these tests were performed on clad plate material and not on actual clad RPVs. For the as-welded condition, two types of residual stress distributions in the cladding were noted by Rybicki.

**Content Deleted -
EPRI Proprietary Information**

**Content Deleted -
EPRI Proprietary Information**

**Content Deleted -
EPRI Proprietary Information**

6.2 Attachment Weld Residual Stresses

The attachment welds shown in Figures 2-2 through 2-7 can be classified into three sets. The first set consists of attachment welds or pads welded directly to the cladding such as the configurations shown in Figures 2-2(a) and 2-2(c). As explained earlier, the cladding had to be qualified as a structural material for this case. The second set consists of the nickel alloy pads welded to the RPV material onto which the attachment weld is fabricated. This is illustrated by the configurations shown in Figure 2-2(b) and the shroud support structure welds to the RPV in Figures 2-3 through 2-6. The third group consists of the nozzle penetration welds illustrated in Figure 2-7. In this report, the residual stress profiles for first two sets of attachment welds are considered.

6.2.1 Attachment Welds and Pads Welded to the Cladding

The residual stress profiles for these attachment welds have not been specifically determined.

**Content Deleted -
EPRI Proprietary Information**

6.2.2 Nickel Alloy Pad Attachment Weld

The fabrication of the nickel alloy pad attachment weld consists of first locally machining a groove through the stainless steel cladding and into the LAS pressure vessel. A pad consisting of weld metal is then deposited in the groove onto the RPV plate using, in most cases, shielded metal arc welding (SMAW) process. The pad is exclusively made of Alloy 182. The bracket is either Alloy 600 or stainless steel. The application of the nickel alloy pad is followed by PWHT of the pad area and the immediate vicinity. The attachment plate is then welded onto the pad, in most cases, using the SMAW process. The attachment weld is not given a PWHT. A photomicrograph of an attachment weld (H9) from the vessel of River Bend plant presented in Reference 6-11 is shown in Figure 6-9.

The residual stress distribution at the nickel alloy pad bracket attachment weld was determined in References 6-10, 6-11 and 6-12.

**Content Deleted -
EPRI Proprietary Information**

**Content Deleted -
EPRI Proprietary Information**

6.3 Vessel Weld Residual

During the fabrication of the vessel, several plates are welded together to form the cylindrical and hemispherical portions before the application of the cladding. The residual stress distributions resulting from the welding of the vessel plates have not been studied extensively.

**Content Deleted -
EPRI Proprietary Information**

6.4 Operating Stresses

In addition to the weld residual stresses, operating stresses need to be considered in the flaw evaluation. These stresses can be obtained from the vessel stress reports for each plant. In the case of old plants, the information in the stress report may not be adequate for this evaluation and therefore an updated stress analysis may have to be performed to support the fracture mechanics evaluation.

**Content Deleted -
EPRI Proprietary Information**

6.5 Fracture Mechanics Stress Intensity Factor Considerations

The load carrying capacity of flawed low alloy ferritic steel can vary significantly within the LWR operating temperature range. This temperature dependence results in three distinct regions, each requiring a different fracture mechanics analysis technique.

1. The “lower shelf” region where the material flaw tolerance is a minimum and does not change significantly with increasing temperature. In this region, the behavior of the material is generally assumed to be linear elastic and therefore, linear elastic fracture mechanics (LEFM) techniques are applicable.
2. The “transition” temperature region where the flaw tolerance increases significantly above the lower shelf value with increasing temperature. In this region, elastic-plastic fracture mechanics (EPFM) techniques involving the use of the J-integral/tearing modulus analyses are typically employed.
3. The “upper shelf” region where the flaw tolerance reaches a maximum and ideally remains constant with increasing temperature. In this region, the material is very ductile and limit load (net section plastic collapse) analyses may be employed in the fracture mechanics evaluation.

**Content Deleted -
EPRI Proprietary Information**

6.5.1 Axial Flaws

To compute the stress intensity factor (axial flaws), a product of an influence function and the stress distribution for the uncracked section is integrated across the crack face:

**Content Deleted -
EPRI Proprietary Information**

6.5.1.1 Stress Intensity Factors for the Clad, Pad and Weld Residual Stress

The stress intensity factors for the clad stress, using the stress distributions in Section 6-1 and Equation 6-1 are shown in Figures 6-11 through 6-13. The stress intensity factors are determined for three clad/vessel thickness ratios of 0.01, 0.02 and 0.05 and peak tensile stress of 138 MPa

(20 ksi) in the clad.

**Content Deleted -
EPRI Proprietary Information**

6.5.1.2 Stress Intensity Factors Due to Operating Stresses

Although Equation (6-1) can also be used to determine the K-distribution for the operating stresses, it is deemed too conservative because it assumes an infinitely long flaw with an aspect ratio (a/t) of zero. While this assumption is necessary to simplify the calculation of the K distribution due to the clad and weld residual stresses, a more realistic model which accounts for finite aspect ratios is used for the K determination of the operating stresses.

**Content Deleted -
EPRI Proprietary Information**

6.5.2 Circumferential Flaws

Equation 6-1 was also used to determine the clad stress K-distribution for circumferential flaws.

**Content Deleted -
EPRI Proprietary Information**

**Content Deleted -
EPRI Proprietary Information**

6.6 References

- 6-1. R. Kume, H. Okabayashi, and T. Naiki, "Internal Stresses in Thick Plates Weld-Overlaid with Austenitic Stainless Steel (Report 1) – Residual Stress Distributions as Welded," *Transaction of the Japan Welding Society*, Vol. 5, No. 1, April 1974, pp.32-38.
- 6-2. W. Bertrem, "Residual Stresses in Weld-Clad Reactor Pressure Vessel Steel," *Transactions of the International Conference on Structural Mechanics in Reactor Technology*, Vol. 3, held in London, England, Sept. 1-5, 1975, paper G 1/9, pp. 1-13.
- 6-3. H. A. Schimmoeller and J. L. Ruge, "Estimation of Residual Stresses in Reactor Pressure Vessel Steel Specimens Clad by Stainless Steel Strip Electrodes," *Proceedings of the International Conference on Residual Stresses in Welded Construction and Their Effects*, held in London, England, Nov. 15-17, 1977, sponsored by the Welding Institute, pp. 251-258.
- 6-4. G. Hofer and N. Bender, "Eigenspannungsmessungen an Plattierungen mit und ohne Spannungsarmgluhen," *DVS Berichte*, Vol. 49, 1978, pp. 18-23
- 6-5. W. Bertrem, "Eigenspannungen in Austenitisch Handplattiertem, Dickwandigen Feinkornbaustahl," Dissertation, Technische Fakultat fur Maschinenbau und Elektrotechnik der Technischen Universitat Carolo-Wilhelmina zu Braunschweig, Braunschweig 1976, S. 55.
- 6-6. F. Eichhorn, G. Hofer, R. Schroder, H. D. Steffens and H. Wohlfahrt, "Residual Stresses in Welded Joints and Sprayed Coatings," *Proceedings of the International Conference on Residual Stresses*, held in Garmisch-Partenkirchen (FRG) by Deutsche Gesellschaft fur Metallkunde, 1987, Vol. 2, pp. 977-987.
- 6-7. E. F. Rybicki, J. R. Shadley, A. S. Sandhu and R. B. Stonesifer, "Experimental and Computational Residual Stress Evaluation of a Weld Clad Plate and Machined Test Specimens," *J. Engineering Materials and Technology*, Vol. 110, Oct. 1988, pp. 297-304.
- 6-8. E. F. Rybicki, J. R. Shadley and A. G. Peterson, Jr., "Experimental Residual Stress Evaluation of a Section of Clad Pressure Vessel Steel," EPRI TR-101989, February 1993.
- 6-9. D. E. McCabe, "Fracture Evaluation of Surface Cracks Embedded in Reactor Vessel Cladding," NUREG/CR-5207 (MEA-2285), September 1988.
- 6-10. W. Cheng and I. Finnie, "The Compliance Method for Measurement of Residual Stresses with Applications to Cladding and Welded Attachment on a Plate," Draft Report, EPRI Project RPC102-2, 1992.

- 6-11. R. J. Dexter, C. P. Leung and D. Pont, "Residual Stress Analysis in BWR Pressure Vessel Attachments," EPRI TR-100651, June 1992.
- 6-12. GE Nuclear Energy Draft Report on EPRI-RP2975-3, "Crack Growth and Fracture Margin Assessment for BWR Attachment Welds," December 1991.
- 6-13. EPRI Draft Report, "Evaluation of Crack Growth in Nickel – Based RPV Internals," October 1998.
- 6-14. D. A. Ferrill, P. B. Juhl and D. R. Miller, "Measurement of Residual Stresses in Heavy Weldment," Welding Research Supplement 507-S, November 1966.
- 6-15. ASME Code, Section XI Working Group on Operating Plant Criteria, "White Paper on Reactor Vessel Integrity Requirements for Level A and B Conditions," EPRI TR-100251, January 1993.
- 6-16. W. A. Logsdon and J. A. Begley, "Dynamic Fracture Toughness of SA 533, Grade A., Class 2 Base Plate and Weldments," Flaw Growth and Fracture ASTM STP 631.
- 6-17. B. H. Menke, et al., "J-Integral, R-Curve Material Characterization," "Evaluation and Prediction of Neutron Embrittlement in Reactor Pressure Vessel Materials," EPRI NP-2782, December 1982.
- 6-18. ASME Boiler and Pressure Vessel Code, Section XI, 1995 Edition
- 6-19. R. Labbens, A. Tatom-Pellisier and J. Heliot, "Practical Method of Calculating Stress Intensity Factors Through Weight Functions," Mechanics of Crack Growth, ASTM STP 590, American Society for Testing and Materials, 1976.
- 6-20. EPRI Document NP-6301-P, "Ductile Fracture Handbook," June 1989.

**Content Deleted -
EPRI Proprietary Information**

Figure 6-1. Average Longitudinal and Transverse Residual Stress Distributions [6-8]

**Content Deleted -
EPRI Proprietary Information**

Figure 6-2. Longitudinal and Transverse Residual Stress Distributions [6-8]

**Content Deleted -
EPRI Proprietary Information**

Figure 6-3. Longitudinal and Transverse Residual Stress Distributions [6-8]

**Content Deleted -
EPRI Proprietary Information**

Figure 6-4. Longitudinal Through-Thickness Residual Stresses in Clad Plate Measured at Position 5.5 in. from Edge [6-9]

**Content Deleted -
EPRI Proprietary Information**

Figure 6-5. Measured Residual Stress in Clad Plate

**Content Deleted -
EPRI Proprietary Information**

Figure 6-6. Residual Circumferential (Longitudinal Stress Due to Stress Relief PWHT from the Simulation of Two Layers of Clad [6-11] (Note 1 MPa = 0.145 ksi)

**Content Deleted -
EPRI Proprietary Information**

Figure 6-7. Variation of Clad Residual Stresses with Temperature

**Content Deleted -
EPRI Proprietary Information**

Figure 6-8. Proposed Clad Residual Stress Profile at Room Temperature

**Content Deleted -
EPRI Proprietary Information**

Figure 6-9. Photomacograph of Weld H9 at River Bend

**Content Deleted -
EPRI Proprietary Information**

Figure 6-10. Residual Stress through RPV Wall below H9 Weld

**Content Deleted -
EPRI Proprietary Information**

Figure 6-11. Stress Intensity Distribution Due to Clad Stress (Axial Flaw - $t_{\text{clad}}/t_{\text{vessel}} = 0.01$)

**Content Deleted -
EPRI Proprietary Information**

Figure 6-12. Stress Intensity Distribution Due to Clad Stress (Axial Flaw - $t_{\text{clad}}/t_{\text{vessel}} = 0.02$)

**Content Deleted -
EPRI Proprietary Information**

Figure 6-13. Stress Intensity Distribution Due to Clad Stress (Axial Flaw - $t_{\text{clad}}/t_{\text{vessel}} = 0.05$)

**Content Deleted -
EPRI Proprietary Information**

Figure 6-14. Stress Intensity Variation for Various Clad to Vessel Thicknesses (Axial Flaw)

**Content Deleted -
EPRI Proprietary Information**

Figure 6-15. Through-wall Stress Intensity Factor Distribution for Vessel Weld Residual Stress (Axial Flaw)

**Content Deleted -
EPRI Proprietary Information**

Figure 6-16. Through-wall Stress Intensity Factor Distribution in a Vessel with Membrane Stress of 10 ksi (Axial Flaw with Aspect Ratio of 0.1 and 0.5)

**Content Deleted -
EPRI Proprietary Information**

Figure 6-17. Through-wall Stress Intensity Factor Distribution in a Vessel with Bending Stress of 10 ksi (Axial Flaw with Aspect Ratio of 0.1 and 0.5)

**Content Deleted -
EPRI Proprietary Information**

Figure 6-18. Cracked Cylinder to Edge-Cracked Plate K_I Curvature Correction Factor for Circumferential Flaws in a Vessel ($t/R = 0.1$)

**Content Deleted -
EPRI Proprietary Information**

Figure 6-19. Stress Intensity Distribution Due to Clad Stress (Circumferential Flaw –
 $t_{\text{clad}}/t_{\text{vessel}} = 0.01$)

**Content Deleted -
EPRI Proprietary Information**

Figure 6-20. Stress Intensity Distribution Due to Clad Stress (Circumferential Flaw –
 $t_{\text{clad}}/t_{\text{vessel}} = 0.02$)

**Content Deleted -
EPRI Proprietary Information**

Figure 6-21. Stress Intensity Distribution Due to Clad Stress (Circumferential Flaw –
 $t_{\text{clad}}/t_{\text{vessel}} = 0.05$)

**Content Deleted -
EPRI Proprietary Information**

Figure 6-22. Stress Intensity for Various Clad to Vessel Thicknesses (Circumferential Flaw)

**Content Deleted -
EPRI Proprietary Information**

Figure 6-23. Through-wall Stress Intensity Factor Distribution for Vessel Weld Residual Stress (Circumferential Flaw)

**Content Deleted -
EPRI Proprietary Information**

Figure 6-24. Through-wall Stress Intensity Factor Distribution in a Vessel with Membrane Stress of 10 ksi (Circumferential Flaw)

**Content Deleted -
EPRI Proprietary Information**

Figure 6-25. Through-wall Stress Intensity Factor Distribution in a Vessel with Bending Stress of 10 ksi (Circumferential Flaw)

**Content Deleted -
EPRI Proprietary Information**

Figure 6-26. Parameter F_t to Describe Stress Intensity Factor K_I for the Part-Through-Wall, Part Circumference Flaws [15]

**Content Deleted -
EPRI Proprietary Information**

Figure 6-27. Flaw Reduction Factors for Determination of K_I for Weld Residual Stresses in BWR Shrouds with Part-Circumference Flaws

7.0 EXAMPLES OF FRACTURE MECHANICS METHODOLOGY FOR RPV AND ATTACHMENTS

Two components are evaluated in this section to illustrate the methodology outlined in the previous sections of this report. The two components chosen for evaluation are:

- Top Head Flange
- Shroud Support Plate

The first component was selected because, in the recent past, flaws have been identified at the locations of this component at BWR plants (see Section 3 of this report). The shroud support plate was chosen for evaluation as a representative of a vessel attachment weld.

7.1 Top Head Cracking Evaluation – Clad Crack Growth Example (Circumferential Flaw)

7.1.1 Background

As reported in Section 3 of this report and further documented in Reference 3-1, inspections were performed on the top head at one BWR during a refueling outage. As a result of these inspections, numerous indications of “rust” were identified inside the vessel head. Further examinations revealed that the cracking existed only in the cladding. The cracking was limited mainly to the manually clad area associated with the RPV head “dollar plate” region, the vessel head and the head flanges and the head-to-flange weld. In these areas, the cladding was applied manually. The indicated areas of rusting mainly followed the circumferential clad weld beads and were most prevalent at the interface between the manual and machine-deposited clad areas. The indications ranged in depth from 3.8 to 5.1 mm (0.15 to 0.20 inches) that would correspond to the thickness of the cladding (nominal thickness = 4.8 mm [0.19 in.]) within the tolerance of the ultrasonic technique and the manual cladding process. The depth of the indications were confirmed near the flange region by grinding of the cladding. It was determined that none of the indications had penetrated into the base material of the vessel head. The approximate location of

the flaws are shown in Figure 7-1. The objective was to perform a fracture mechanics evaluation to determine suitability for continued operation with the observed indications.

**Content Deleted -
EPRI Proprietary Information**

7.1.2 Stresses

Because of the location of the flaw, the following stresses were considered in the analysis:

**Content Deleted -
EPRI Proprietary Information**

**Content Deleted -
EPRI Proprietary Information**

7.1.3 *Stress Intensity Factors*

**Content Deleted -
EPRI Proprietary Information**

**Content Deleted -
EPRI Proprietary Information**

7.1.4 Stress Corrosion Crack Growth Evaluation

**Content Deleted -
EPRI Proprietary Information**

**Content Deleted -
EPRI Proprietary Information**

7.1.5 Allowable Flaw Size

**Content Deleted -
EPRI Proprietary Information**

7.2 H-9 Attachment Weld – Crack Growth Example (Circumferential Flaw)

7.2.1 Background

This example is for illustrative purposes only and does not represent any identified flawed condition in a BWR. It was chosen because unlike the vessel head, the interaction of the shroud support plate with the vessel introduces significant secondary stresses in the local region of the vessel. The vessel chosen is a BWR-4. The geometry of the configuration is shown in Figure 7-5 with further details provided in Figure 7-6. The vessel has an inside radius of 2.816m (110.875 inches) and thickness of 136.5 mm (5.375 inches) at the H-9 weld. The cladding thickness is 3.1 mm (0.125 inch) resulting in a clad to vessel thickness ratio of 0.023. The assumed location of the flaw is shown in Figure 7-5.

7.2.2 Stresses

Stress considered in the evaluation consisted of

**Content Deleted -
EPRI Proprietary Information**

**Content Deleted -
EPRI Proprietary Information**

7.2.3 *Stresses Intensity Factors*

**Content Deleted -
EPRI Proprietary Information**

7.2.4 *Stress Corrosion Crack Growth Evaluation*

The stress corrosion crack growth was performed in a consistent fashion with the previous example. The results evaluation are presented in Figure 7-8.

**Content Deleted -
EPRI Proprietary Information**

7.3 *Examples with Axial Flaws*

The above two examples involved the assumption of a circumferential flaw. In this section, axial flaws are assumed at the same locations as in these examples.

**Content Deleted -
EPRI Proprietary Information**

7.4 References

- 7-1. Structural Integrity Associates, **pc-CRACK** for Windows, Version 3.0-3/27/97.

Table 7-1

Load Case 1

Preload + Pressure = 0

**Content Deleted -
EPRI Proprietary Information**

Table 7-2

Load Case 2

Preload + Pressure = 1250 psi

**Content Deleted -
EPRI Proprietary Information**

Table 7-3

Load Case 3

Start-up Transient, Pressure = 1000 psi

**Content Deleted -
EPRI Proprietary Information**

Table 7-4
Load Case 4
Cooldown Transient, Pressure = 34.1 psi

**Content Deleted -
EPRI Proprietary Information**

Table 7-5
Steady State Stresses at Weld H-9

**Content Deleted -
EPRI Proprietary Information**

Table 7-6
Hydrotest Stresses at Weld H-9

**Content Deleted -
EPRI Proprietary Information**

**Content Deleted -
EPRI Proprietary Information**

Figure 7-1. Reactor Vessel Head and Flange

**Content Deleted -
EPRI Proprietary Information**

Figure 7-2. Vessel Head Stress Distribution

**Content Deleted -
EPRI Proprietary Information**

Figure 7-3. Allowable Flaw Size Determination for Vessel Head (360° Flaw)

**Content Deleted -
EPRI Proprietary Information**

Figure 7-4. Stress Corrosion Cracking Evaluation Results (Circumferential Flaw) for Vessel Head

**Content Deleted -
EPRI Proprietary Information**

Figure 7-5. Configuration of Vessel at Weld H9 (Shroud Support Plate to Vessel)

**Content Deleted -
EPRI Proprietary Information**

Figure 7-6. Details of Vessel Configuration at Weld H9

**Content Deleted -
EPRI Proprietary Information**

Figure 7-7. Allowable Flaw Size Determination for Vessel Near Weld H-9 (360° Flaw)

**Content Deleted -
EPRI Proprietary Information**

Figure 7-8. Stress Corrosion Cracking Evaluation Results for Vessel Near Weld H-9 (Circumferential Flaw)

**Content Deleted -
EPRI Proprietary Information**

Figure 7-9. Allowable Flaw Size Determination for Vessel Head (Axial Flaw)

**Content Deleted -
EPRI Proprietary Information**

Figure 7-10. Stress Corrosion Crack Growth for Vessel Head and Comparison to Allowable (Axial Flaw)

**Content Deleted -
EPRI Proprietary Information**

Figure 7-11. Allowable Flaw Size Determination for Vessel Weld Near H-9 (Axial Flaw)

**Content Deleted -
EPRI Proprietary Information**

Figure 7-12. Stress Corrosion Crack Growth for Vessel Weld New Weld H-9 (Axial Flaw)

8.0 SUMMARY AND CONCLUSIONS

The following provides a summary and conclusions of the work performed in this report to support crack growth evaluation in low alloy steel vessel materials in the BWR environment.

**Content Deleted -
EPRI Proprietary Information**

**Content Deleted -
EPRI Proprietary Information**

**Content Deleted -
EPRI Proprietary Information**

TECHNICAL SERVICES
GENE-B13-01920-066
Class III
February 1999

Appendix A:

EPRI RPC102-4: Stress Corrosion Cracking in Low Alloy Steels: Task 4: Reactor Site Verification Test

Prepared for

EPRI

Prepared by

**GE Nuclear Energy
175 Curtner Avenue
San Jose, CA 95125**

**EPRI RPC102-4: Stress Corrosion Cracking in
Low Alloy Steels:
Task 4: Reactor Site Verification Test**

February 1999

Prepared by: _____
R. M. Horn, Engineering Fellow
Materials Technology

Prepared by: _____
D. A. Hale, Technical Expert: CAV Testing
BWR Technology

Approved by: _____
T. A. Caine, Manager
Structural Mechanics and Materials

IMPORTANT NOTICE REGARDING
CONTENTS OF THIS REPORT

Please read carefully

The only undertakings of the General Electric Company (GE) respecting information in this document are contained in the contract between EPRI and GE, and nothing contained in this document shall be construed as changing the contract. The use of this information by anyone other than EPRI with respect to any unauthorized use, GE makes no representation or warranty, express or implied, and assumes no liability as to the completeness, accuracy, or usefulness of the information contained in this document, or that its use may not infringe upon privately owned rights.

TABLE OF CONTENTS

BACKGROUND	1
TEST DESIGN AND PURPOSE	2
TEST MATERIALS AND PREPARATION	3
CAV AUTOCLAVE AND TESTING SETUP	3
REACTOR SITE TESTING	4
PLANT CHEMISTRY	4
ECP MEASUREMENTS	5
LOADING HISTORY	5
CRACK GROWTH RESULTS	5
<i>Specimen LAS 89: "High Sulfur" Material</i>	6
<i>Specimen LAS 88</i>	7
<i>Specimen LAS 90: Low Sulfur Material</i>	7
DISCUSSION OF RESULTS	8
ROLE OF MATERIAL CHEMISTRY, WATER CHEMISTRY AND LOADING HISTORY	8
<i>Material Chemistry</i>	8
<i>Water Chemistry</i>	8
<i>Loading Effects</i>	9
COMPARISON WITH OTHER LOW ALLOY STEEL DATA	9
CONCLUSIONS	9
REFERENCES	10
ACKNOWLEDGMENTS	10

Background

**Content Deleted -
EPRI Proprietary Information**

**Content Deleted -
EPRI Proprietary Information**

Test Design and Purpose

**Content Deleted -
EPRI Proprietary Information**

Test Materials and Preparation

**Content Deleted -
EPRI Proprietary Information**

CAV Autoclave and Testing Setup

**Content Deleted -
EPRI Proprietary Information**

**Content Deleted -
EPRI Proprietary Information**

Reactor Site Testing

**Content Deleted -
EPRI Proprietary Information**

Plant Chemistry

**Content Deleted -
EPRI Proprietary Information**

**Content Deleted -
EPRI Proprietary Information**

ECP Measurements

**Content Deleted -
EPRI Proprietary Information**

Loading History

**Content Deleted -
EPRI Proprietary Information**

Crack Growth Results

**Content Deleted -
EPRI Proprietary Information**

**Content Deleted -
EPRI Proprietary Information**

**Content Deleted -
EPRI Proprietary Information**

Discussion of Results

Role of Material Chemistry, Water Chemistry and Loading History

**Content Deleted -
EPRI Proprietary Information**

**Content Deleted -
EPRI Proprietary Information**

Comparison with Other Low Alloy Steel Data

**Content Deleted -
EPRI Proprietary Information**

Conclusions

**Content Deleted -
EPRI Proprietary Information**

Content Deleted - EPRI Proprietary Information

References

A-1. "Stress Corrosion Cracking in Low Alloy Steels, Interim Technical Report," prepared for EPRI by GE Nuclear Energy on EPRI Contract No. RP C102-4, dated February 1994.

A-2. K. Kussmaul, D. Blind and V. Laepple, "New Observations on the crack growth of low alloy nuclear grade ferritic steels under constant active load in oxygenated high-temperature water," Nuclear Eng. and Design, 168, pp53-75, 1997.

Acknowledgments

Several acknowledgments are appropriate. First, and foremost, the Iberdrola Utility management must be thanked for their support of the test program at Cofrentes. Señor Juan de Dios Sanchez Zapata, the Chemistry Supervisor at Cofrentes, was also key to conducting the test and to transferring the test data for analysis. Andy Unruh was responsible for the majority of the testing. Finally, Dan Weinstein, the GE International team in Spain, and the EPRI sponsorship under the lead of Dr. Larry Nelson and Dr. Raj Pathania were also critical to the project initiation and completion.

Table A-1: Compositions of the Low Alloy Steel Specimens (wt. %)

**Content Deleted -
EPRI Proprietary Information**

Table A-2: Summary of Different Test Time Periods

**Content Deleted -
EPRI Proprietary Information**

**Table A-3: Crack Growth Results:
(Crack Growth Rates in mm/s and in/h)**

**Content Deleted -
EPRI Proprietary Information**

Table A-4: Crack Growth Results:
(Crack Growth Rates in average mm/y and mils/y)

**Content Deleted -
EPRI Proprietary Information**

**Content Deleted -
EPRI Proprietary Information**

Figure A-1. Summary of Results of Round Robin Test

**Content Deleted -
EPRI Proprietary Information**

**Figure A-2. Crack Growth of Low Alloy Steel: Four Phases of
Loading in GENE Eight Specimen Test**

**Content Deleted -
EPRI Proprietary Information**

**Figure A-3. Schematic of Potential Drop Wiring on 1T Compact Tension (CT) Specimen
Used to Measure Crack Growth in Low Alloy steel Materials in CAVS System**

**Content Deleted -
EPRI Proprietary Information**

**Figure A-4. CAV Load Frame Showing Crack Growth Vessel and Small ECP Autoclave
(Note: Majority of Loading Attributed Dead Weight Load Applied through Lever Arm)**

**Content Deleted -
EPRI Proprietary Information**

Figure A-5: Photograph of Low Alloy Steel specimens in CAV load chain. Redundant potential drop leads clearly visible.

**Content Deleted -
EPRI Proprietary Information**

Figure A-6: The Overview of the assembled CAV test system, ready to be shipped to site.

**Content Deleted -
EPRI Proprietary Information**

Figure A-7: Plant Power over the period of Low Alloy Steel Testing.

**Content Deleted -
EPRI Proprietary Information**

Figure A-8: CAVS Autoclave Inlet temperature over the Low Alloy Steel test period.

**Content Deleted -
EPRI Proprietary Information**

Figure A-9: Measured conductivity over the Low Alloy Steel test period.

**Content Deleted -
EPRI Proprietary Information**

Figure A-10: ECP Measurements for Low Alloy Steel over test period.

**Content Deleted -
EPRI Proprietary Information**

Figure A-11: The calculated stress intensity as a function of time for the Low Alloy Steel specimens.

**Content Deleted -
EPRI Proprietary Information**

Figure A-12: Crack length as a function of time for specimen LAS 89

**Content Deleted -
EPRI Proprietary Information**

**Figure A-13: Crack length as a function of time for first 1100 hours
of exposure: Specimen LAS 89**

**Content Deleted -
EPRI Proprietary Information**

Figure A-14: Crack length as a function of time for specimen LAS 88

**Content Deleted -
EPRI Proprietary Information**

**Figure A-15: Crack length as a function of time for first 1100 hours
of exposure: Specimen LAS 88**

**Content Deleted -
EPRI Proprietary Information**

Figure A-16: Crack length as a function of time for specimen LAS 90

**Content Deleted -
EPRI Proprietary Information**

**Figure A-17: Crack length as a function of time for first 1100 hours
of exposure: Specimen LAS 90**

**Content Deleted -
EPRI Proprietary Information**

Figure A-18. CAV crack growth rates plotted for each material and test period. The rates in periods 5, 6 and 7 are very low, nearing the resolution limit.

**Content Deleted -
EPRI Proprietary Information**

Figure A-19. Average crack growth rates in the LAS CAV specimens plotted for normal water chemistry but a function of the two reload frequencies

**Content Deleted -
EPRI Proprietary Information**

Figure A-20. Apparent crack growth rates determined by MPA-Stuttgart together with their chosen bounding line and the GE theoretical lines. Note that the bounding line at the lower K values is set by 1000 hr test time data.


Targets:
Nuclear Power

About EPRI

EPRI creates science and technology solutions for the global energy and energy services industry. U.S. electric utilities established the Electric Power Research Institute in 1973 as a nonprofit research consortium for the benefit of utility members, their customers, and society. Now known simply as EPRI, the company provides a wide range of innovative products and services to more than 1000 energy-related organizations in 40 countries. EPRI's multidisciplinary team of scientists and engineers draws on a worldwide network of technical and business expertise to help solve today's toughest energy and environmental problems.

EPRI. Powering Progress

© 2000 Electric Power Research Institute (EPRI), Inc. All rights reserved. Electric Power Research Institute and EPRI are registered service marks of the Electric Power Research Institute, Inc. EPRI. POWERING PROGRESS is a service mark of the Electric Power Research Institute, Inc.

 Printed on recycled paper in the United States of America

TR-108709NP